

2000

Technicolor signatures---ieri, oggi e domani

Kenneth Lane. 2000. "Technicolor Signatures---ieri, Oggi e Domani." <http://arxiv.org/abs/hep-ph/0006143v2>
<https://hdl.handle.net/2144/40101>

"Downloaded from OpenBU. Boston University's institutional repository."

TECHNICOLOR SIGNATURES—IERI, OGGI E DOMANI

KENNETH LANE

*Department of Physics, Boston University
590 Commonwealth Avenue, Boston, Massachusetts 02215*

Abstract

We briefly review the basic structure of modern-day technicolor theories. We then discuss the signatures for technicolor as they were in its early days, the searches that have been recently performed at the Tevatron and LEP colliders, and the prospects for testing technicolor in Tevatron Run II and at the LHC.

1. Introduction

Since the standard model was constructed in the first half of the 1970s, there has been discomfort and dissatisfaction with one of its foundations, the description of electroweak and flavor symmetry breaking in terms of one or more elementary Higgs boson multiplets. This is no description at all. No dynamical reason is provided for electroweak symmetry breaking. There is no understanding of why its energy scale is roughly 1 TeV and, in particular why it is so much less than the GUT scale, if there is one, or the Planck scale if there isn't. This is the hierarchy problem. Another difficulty is the naturalness problem. ¹⁾ Why should the Higgs mass, which suffers quadratic renormalization, be very much less than the natural cutoff of the theory, the GUT scale or the Planck scale? Furthermore, in all elementary Higgs models, every aspect of flavor—from the primordial symmetry that tells us the number of quark and lepton generations to the weird pattern of flavor breaking—is completely arbitrary, put in by hand. Finally, it is now well understood that elementary Higgs models are “trivial”, i.e., they become free field theories in the limit of infinite cutoff. ²⁾ This means that these models are at best effective, describing a more fundamental theory that must be used above some finite energy. If the Higgs boson is light, less than 200–300 GeV, this transition to a more fundamental theory may be postponed until very high energy, but what lies up there worries us nonetheless.

In response to these shortcomings, the dynamical picture of electroweak and flavor symmetry breaking emerged in 1978–80. This picture, now known as technicolor (TC) ^{3, 4, 5, 6)} and extended technicolor (ETC), ^{7, 8)} was motivated first of all by the premise that *every* fundamental energy scale should have a dynamical origin. Thus, the weak scale (or vacuum expectation value of the Higgs field) $v = 2^{-1/4}G_F^{-1/2} = 246 \text{ GeV}$ should reflect the fundamental scale of a new strong dynamics, technicolor, just as the pion decay constant $f_\pi = 93 \text{ MeV}$ reflects QCD's scale of about 200 MeV. For this reason, I write $F_\pi = 2^{-1/4}G_F^{-1/2} = 246 \text{ GeV}$ to emphasize its dynamical origin.

Technicolor, a gauge theory of fermions with no elementary scalars, is modeled on the precedent of QCD. In QCD, massless quarks have a chiral symmetry that is spontaneously broken, giving rise to massless Goldstone bosons, the pions. When this happens in technicolor, three Goldstone bosons become, via the Higgs mechanism, the longitudinal components W_L^\pm and Z_L^0 of the weak bosons. With technifermions forming left-handed doublets and right-handed singlets under electroweak $SU(2) \otimes U(1)$, the electroweak masses are $M_W = M_Z \cos \theta_W = \frac{1}{2}gF_\pi$, where $g = e/\sin \theta_W$.

Like QCD, technicolor is asymptotically free. This solves in one stroke the naturalness, hierarchy, and triviality problems. If we imagine that the technicolor gauge symmetry (taken here to be $SU(N_{TC})$) is embedded at a very high energy Λ in some grand unified gauge group, then TC's characteristic scale Λ_{TC} , where the coupling α_{TC} becomes strong enough to trigger chiral symmetry breaking, is naturally exponentially smaller than Λ . The mass of all technihadrons, including Higgs-like scalars (though that language is neither accurate nor useful in technicolor) is of order Λ_{TC} . And asymptotically free field theories are nontrivial. No other scenario for the physics of the TeV scale solves these problems so neatly. Period.

Technicolor alone cannot address the flavor problem. Something more is needed to communicate electroweak symmetry breaking to quarks and leptons and give them mass. Furthermore, in all but the minimal TC model with a single doublet of technifermions, there are Goldstone bosons—technipions π_T , in addition to W_L^\pm and Z_L^0 —that must be given mass. Their masses must be more than 50–100 GeV for these π_T to have escaped detection. Extended technicolor was invented to address these and other aspects of flavor physics. It was also motivated by the desire to make flavor understandable at energies well below the GUT scale in terms of gauge dynamics of the kind that worked so neatly for electroweak symmetry breaking, namely, technicolor.

In extended technicolor, the ordinary $SU(3)$ color, $SU(N_{TC})$ technicolor, and flavor symmetries are unified into a larger ETC gauge group. This symmetry is broken down at a scale of 100s of TeV into $SU(3) \otimes SU(N_{TC})$. The ETC interactions must break explicitly all *global* flavor symmetries. The broken gauge interactions are mediated by massive ETC boson exchange and they connect technifermions to each other, giving mass to technipions, and to quarks and leptons, giving mass to them. Generic expressions for technipion masses in terms of four-technifermion condensate renormalized at the ETC scale are

$$F_T^2 M_{\pi_T}^2 \simeq 2 \frac{g_{ETC}^2}{M_{ETC}^2} \langle \bar{T}_L T_R \bar{T}_R T_L \rangle_{ETC}. \quad (1)$$

Here, F_T is the technipion decay constant. In TC models containing N doublets of color-singlet technifermions, $F_T = F_\pi/\sqrt{N}$. Typical quark and lepton masses are given by

$$m_q(M_{ETC}) \simeq m_\ell(M_{ETC}) \simeq \frac{g_{ETC}^2}{2M_{ETC}^2} \langle \bar{T}T \rangle_{ETC}, \quad (2)$$

where $\langle \bar{T}T \rangle_{ETC}$ is the bilinear technifermion condensate renormalized at M_{ETC} . This is related to the condensate renormalized at Λ_{TC} , expected by scaling from

QCD to be

$$\langle \bar{T}T \rangle_{TC} \simeq 4\pi F_T^3, \quad (3)$$

by

$$\langle \bar{T}T \rangle_{ETC} = \langle \bar{T}T \rangle_{TC} \exp \left(\int_{\Lambda_{TC}}^{M_{ETC}} \frac{d\mu}{\mu} \gamma_m(\mu) \right). \quad (4)$$

The anomalous dimension γ_m of the operator $\bar{T}T$ is given in perturbation theory by

$$\gamma_m(\mu) = \frac{3C_2(R)}{2\pi} \alpha_{TC}(\mu) + O(\alpha_{TC}^2), \quad (5)$$

where $C_2(R)$ is the quadratic Casimir of the technifermion $SU(N_{TC})$ -representation R . For the fundamental representation of $SU(N_{TC})$, $C_2(N_{TC}) = (N_{TC}^2 - 1)/2N_{TC}$.

Extended technicolor, like *all* other attempts to understand flavor, has met many obstacles and there is still no “standard ETC” model. This is perhaps not surprising since ETC is essentially a problem in strongly coupled dynamics. Thus, from the beginning, we (few) technicolor enthusiasts have pushed hard for experimental tests of its basic ideas. In the rest of this paper, I will review and preview those searches for technicolor.

2. Yesterday

At the very beginning of technicolor, Susskind proposed one of its most enduring signals. ³⁾ In any model of technicolor, one expects bound technihadrons with a spectrum of mesons paralleling what we see in QCD. These will include spin-zero technipions and spin-one isovector technirhos and isoscalar techniomegas. In the minimal one-technidoublet model ($T = (T_U, T_D)$), the technipions are, by virtue of the Higgs mechanism, the longitudinal components W_L of the massive weak gauge bosons. Susskind pointed out that the analog of the QCD decay $\rho \rightarrow \pi\pi$ is $\rho_T \rightarrow W_L W_L$. In the limit that $M_{\rho_T} \gg M_{W,Z}$, the equivalence theorem states that the amplitude for $\rho_T \rightarrow W_L W_L$ has the same form as the one for $\rho \rightarrow \pi\pi$. If one scales TC from QCD using large- N_{TC} arguments, it is easy to estimate the strength of this amplitude and the ρ_T mass and decay rate ⁹⁾:

$$\begin{aligned} M_{\rho_T} &= \sqrt{\frac{3}{N_{TC}}} \frac{F_\pi}{f_\pi} M_\rho \simeq 2\sqrt{\frac{3}{N_{TC}}} \text{TeV}, \\ \Gamma(\rho_T \rightarrow W_L W_L) &= \frac{2\alpha_{\rho_T} p_W^3}{3M_{\rho_T}^2} \simeq 500 \left(\frac{3}{N_{TC}} \right)^{3/2} \text{GeV}. \end{aligned} \quad (6)$$

Here, the naive scaling argument gives $\alpha_{\rho_T} = (3/N_{TC})\alpha_\rho$ where $\alpha_\rho = 2.91$.

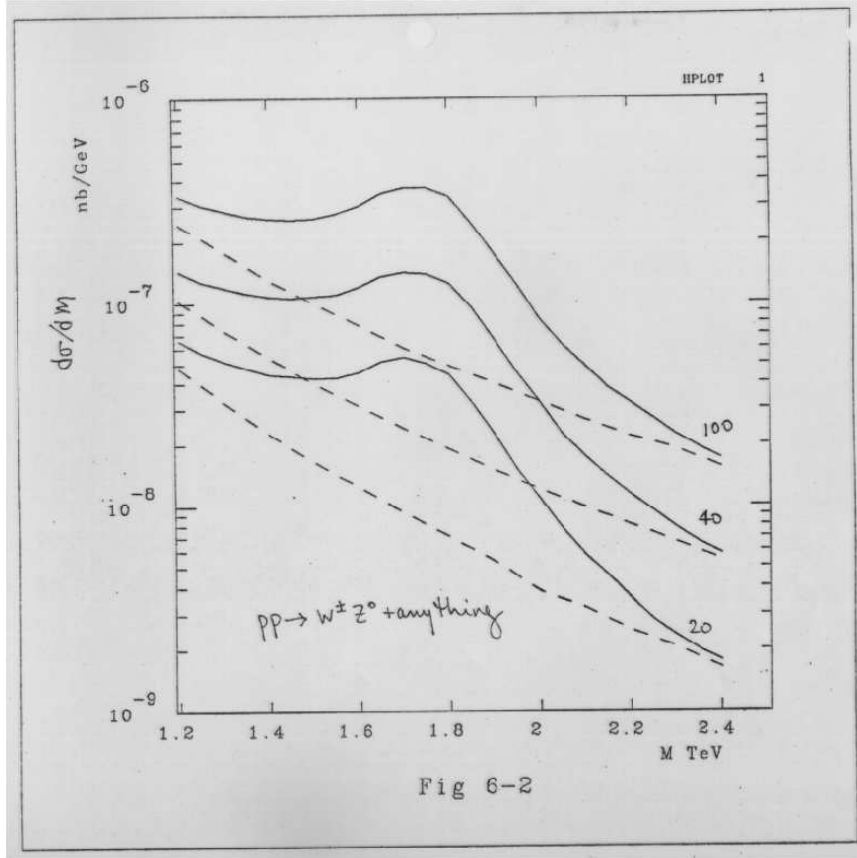


Figure 1: *Mass spectrum in pp collisions at $\sqrt{s} = 20, 40, 100$ TeV for $\rho_T^\pm \rightarrow W^\pm Z^0$ with $M_{\rho_T} = 1.75$ TeV. Dashed lines show the standard model contribution; from Ref. [9].*

For a long time this was the “benchmark” signature for technicolor—the analog of the search for the standard model Higgs for $M_H \simeq 100\text{--}800$ GeV—and some effort has gone into establishing the reach of hadron and lepton colliders for this process. The first accurate calculation (i.e., with standard model interference) was carried out at the parton level in EHLQ for the Superconducting Super Collider with $\sqrt{s} = 10\text{--}100$ TeV. ⁹⁾ Unfortunately, the SSC was cancelled before detailed (particle level) simulations could be carried out and all that was done is exemplified in Fig. 1 for $\rho_T^\pm \rightarrow W^\pm Z^0$ with $M_{\rho_T} = 1.75$ TeV (i.e., $N_{TC} = 4$). CERN’s Large Hadron Collider has no reach for such a heavy ρ_T , as can be seen in Fig. 2. ¹⁰⁾ That, in fact, is why the 40 TeV energy and $10^{33}\text{--}10^{34}$ luminosity were chosen for the SSC.

The high energy lepton collider that has studied its reach for $\rho_T^0 \rightarrow W_L^+ W_L^-$

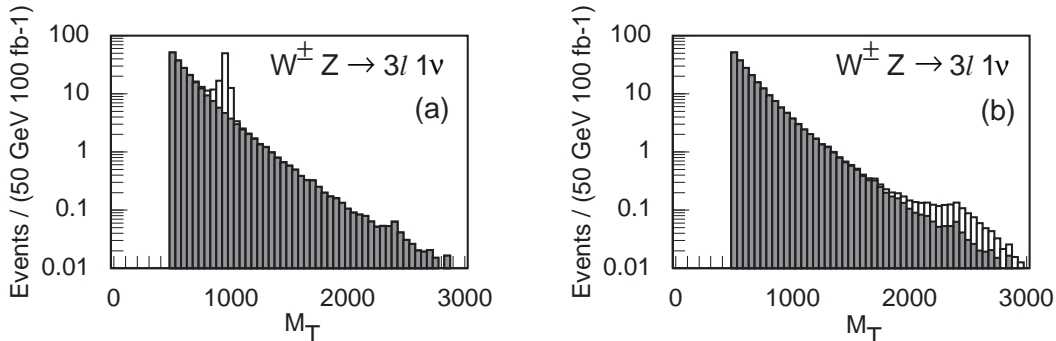


Figure 2: *Event yields at the LHC for $\rho_T^\pm \rightarrow W^\pm Z^0 \rightarrow \ell^\pm \nu_\ell \ell^+ \ell^-$ for $M_{\rho_T} = 1.0, 2.5$ TeV; from Ref. [10].*

is the Next Linear Collider. ¹¹⁾ As currently designed, the NLC reaches to 500 GeV, extendible to 1 TeV. Having no direct reach for a minimal technicolor ρ_T with the expected mass, the NLC relies on probing the form factor in W^+W^- production at $s \ll M_{\rho_T}^2$. In Fig. 3, for a linear collider with $\sqrt{s} = 500$ GeV, a reach up to $M_{\rho_T} \simeq 2$ TeV at the 95% confidence level is indicated. This is about as heavy as one would expect a minimal-model ground state technirho to be. Of course, one would not be satisfied until it were directly observed as an s -channel resonance. Since we still do not know the dynamics underlying electroweak symmetry breaking, this is one of the reasons that the NLC (which will come on well after the LHC anyway) needs to have an energy of at least 1.5–2 TeV. In any case, the 40 TeV high-luminosity SSC was and still is the right collider to build. Alas, that is politically impossible.

It is possible that, like the search for the minimal standard model Higgs boson, all this emphasis on the $W_L W_L$ decay mode of the ρ_T is somewhat misguided. ⁴⁾ Since the minimal ρ_T is so much heavier than $2M_W$, this decay mode may be suppressed by the high W -momentum in the decay form factor. Then, ρ_T decays to four or more weak bosons may be competitive or even dominate. This means that the minimal ρ_T may be wider than indicated in Eq. (6) and, in any case, that its decays are much more complicated than previously thought. Furthermore, walking technicolor, ¹²⁾ discussed below, implies that the spectrum of technihadrons cannot be exactly QCD-like. Rather, there must be something like a tower of technirhos extending almost up to $M_{ETC} \gtrsim$ several 100 TeV. Whether or not these would appear as discernible resonances is an open question. ¹³⁾ All these remarks apply as well to the isoscalar ω_T and its excitations.

As everyone knows, technicolor and extended technicolor are challenged by

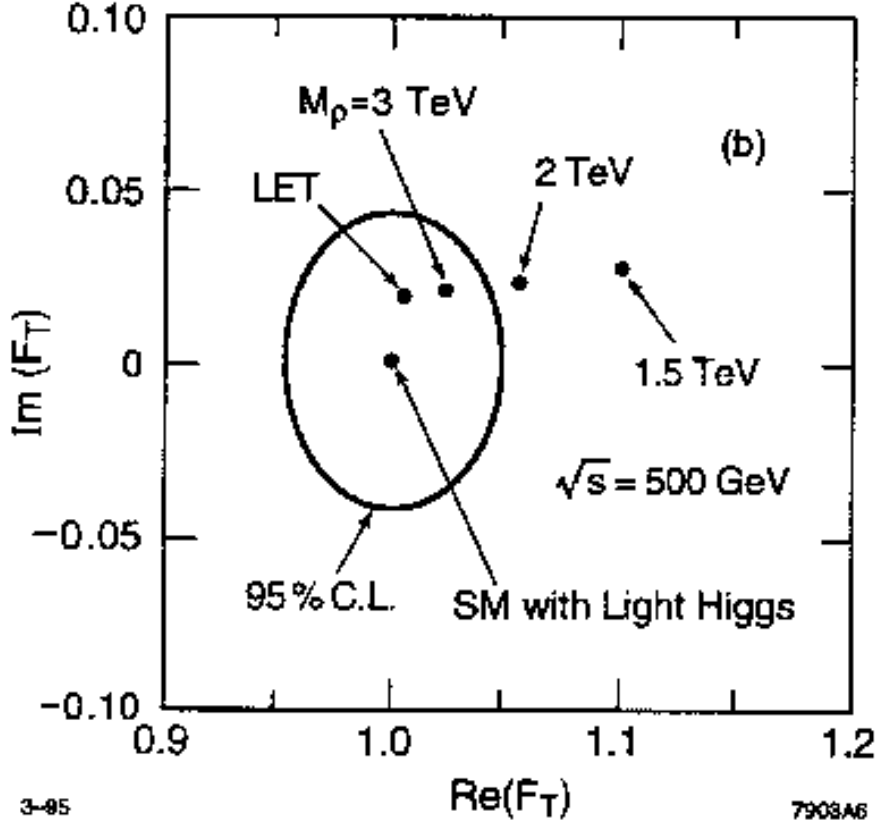


Figure 3: Sensitivity of a 500 GeV NLC to M_{ρ_T} via the W -boson form factor; from Ref. [11].

flavor-changing neutral current interactions (FCNC), ⁷⁾ by precision measurements of electroweak quantities (STU), ¹⁴⁾ and by the large mass of the top quark. In general, we expect four-quark contact interactions generated by ETC exchange. Even if these are generation-conserving to start with, quark mixing is bound to result in $|\Delta S| = 2$ terms with strength $g_{ETC}^2 V_{ds}^2 / M_{ETC}^2$. Here, V_{ds} is a mixing angle factor, presumed to be of order 0.1. The K_L - K_S mass difference and the CP-violating parameter ϵ imply the constraints ^{7, 4, 6)}

$$\frac{M_{ETC}}{g_{ETC} \sqrt{\text{Re}(V_{ds}^2)}} \gtrsim 1300 \text{ TeV}, \quad \frac{M_{ETC}}{g_{ETC} \sqrt{\text{Im}(V_{ds}^2)}} \gtrsim 16000 \text{ TeV}. \quad (7)$$

If we naively scale the technifermion condensates in Eqs. (1,2) from QCD, i.e., assume the anomalous dimension γ_m is small so that $4\langle \bar{T}_L T_R \bar{T}_R T_L \rangle_{ETC} \simeq \langle \bar{T} T \rangle_{ETC}^2 \simeq \langle \bar{T} T \rangle_{TC}^2 \simeq (4\pi F_T^3)^2$, we obtain technipion and quark and lepton masses that are at least 10–1000 times too small, depending on the size of V_{ds} . This is the FCNC problem. It is remedied by the non-QCD-like dynamics of technicolor with a slowly

running gauge coupling, “walking technicolor”, which will be described in the next section.

Precision electroweak measurements actually challenge technicolor, not extended technicolor. The most cited constraint involves the so-called S parameter whose measured value is $S = -0.07 \pm 0.11$ (for $M_H = 100$ GeV).¹⁵⁾ The value obtained in technicolor by scaling from QCD is $\mathcal{O}(1)$. For example, for N color-singlet technidoublets, Peskin and Takeuchi found¹⁴⁾

$$S = 4\pi \left(1 + \frac{M_{\rho_T}^2}{M_{a_{1T}}^2} \right) \frac{F_\pi^2}{M_{\rho_T}^2} \simeq 0.25 N \frac{N_{TC}}{3}. \quad (8)$$

The resolution to this problem may also be found in walking technicolor. One thing is sure: naive scaling of S from QCD is unjustified and probably incorrect in walking gauge theories. No reliable estimate exists because no data on walking gauge theories is available to put into S 's calculation.

The large top quark mass requires a different dynamical innovation than walking technicolor. Extended technicolor cannot explain the top quark's mass without running afoul of either experimental constraints from the parameter $\rho = M_W^2/M_Z^2 \cos^2 \theta_W$ and the $Z \rightarrow \bar{b}b$ decay rate¹⁶⁾—the ETC mass must be about 1 TeV to produce $m_t = 175$ GeV; see Eq. (2)—or of cherished notions of naturalness— M_{ETC} may be higher, but the coupling g_{ETC} then must be fine-tuned near to a critical value. The best idea to explain the top mass so far is topcolor-assisted technicolor,¹⁷⁾ in which a new gauge interaction, topcolor,¹⁸⁾ becomes strong near 1 TeV and generates a large $\bar{t}t$ condensate and top mass. This, too, will be described in the next section.

3. Today

Theoretical Issues: Walking Technicolor and Topcolor-Assisted Technicolor

The FCNC and STU difficulties of technicolor have a common cause: the assumption that technicolor is just a scaled-up version of QCD. In a QCD-like technicolor theory, asymptotic freedom sets in quickly above Λ_{TC} , $\gamma_m \ll 1$, and $\langle \bar{T}T \rangle_{ETC} \simeq \langle \bar{T}T \rangle_{TC}$. The conclusion that fermion and technipion masses are one or more orders of magnitude too small then follows from the requirement in Eq. (7) that $M_{ETC} > 100$ TeV. Scaling from QCD also means that the technihadron spectrum is just a magnified image of the QCD-hadron spectrum, hence that S is too large for all technicolor models except, possibly, the minimal one-doublet model with $N_{TC} \lesssim 4$. A solution to these difficulties in a technicolor theory lies in gauge dynamics that are

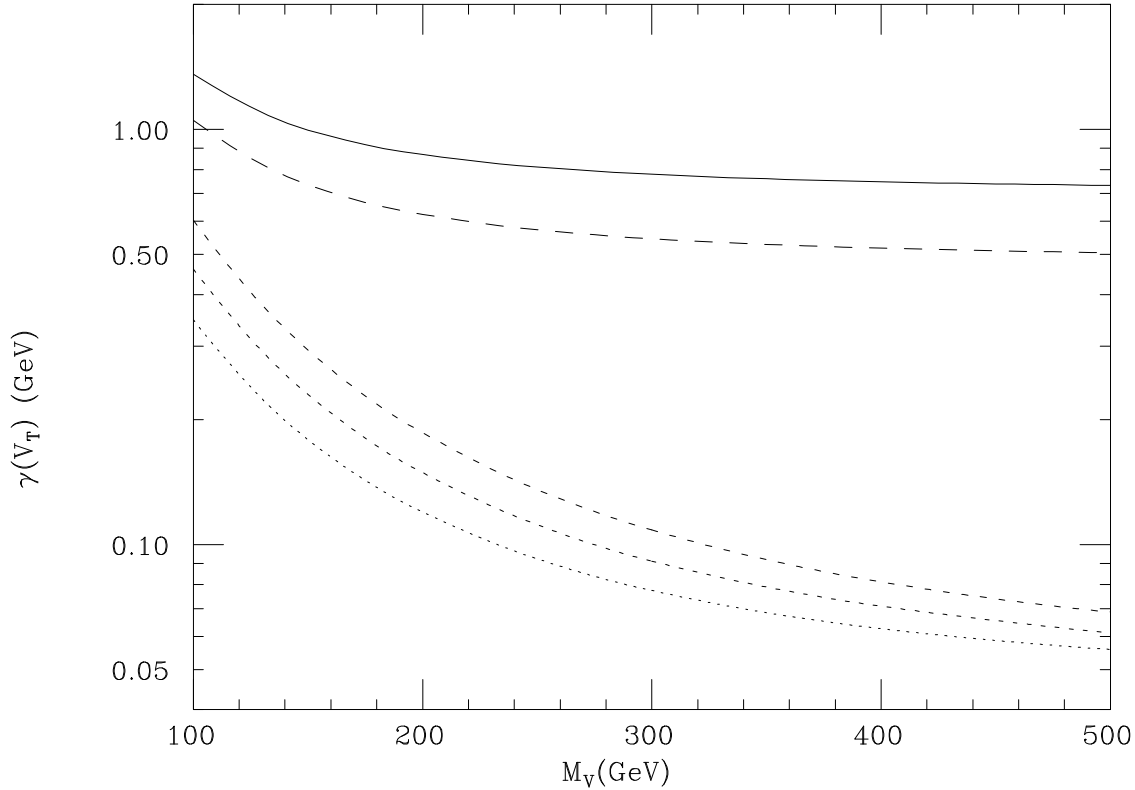


Figure 4: *Technivector meson decay rates versus $M_V = M_A$ for ρ_T^0 (solid curve) and ρ_T^\pm (long-dashed) with $M_{\rho_T} = 210$ GeV, and ω_T with $M_{\omega_T} = 200$ (lower dotted), 210 (lower short-dashed), and 220 GeV (lower medium-dashed); $Q_U + Q_D = 5/3$ and $M_{\pi_T} = 110$ GeV; from Ref. [26].*

distinctly not QCD-like. A technicolor theory in which the gauge coupling evolves slowly, or “walks”, is the only promising example of this. ¹²⁾

In walking technicolor, the gauge coupling $\alpha_{TC}(\mu)$ remains close to its critical value, the one required for spontaneous chiral symmetry breaking, for scales $\Lambda_{TC} < \mu \lesssim M_{ETC}$. This implies that the anomalous dimension $\gamma_m(\mu) \simeq 1$ in Eq. (4), enhancing the condensate $\langle \bar{T}T \rangle_{ETC}$ by a factor of 100 or more. This yields quark masses up to a few GeV and reasonably large technipion masses despite the very large ETC mass scale. This is still not enough to account for the top mass; more on that momentarily.

Another consequence of the walking α_{TC} is that the spectrum of technihadrons, especially ρ_T and ω_T , cannot be QCD-like. ^{4, 19)} If it were, the integrals appearing in Weinberg’s spectral function sum rules ²⁰⁾ would converge much more

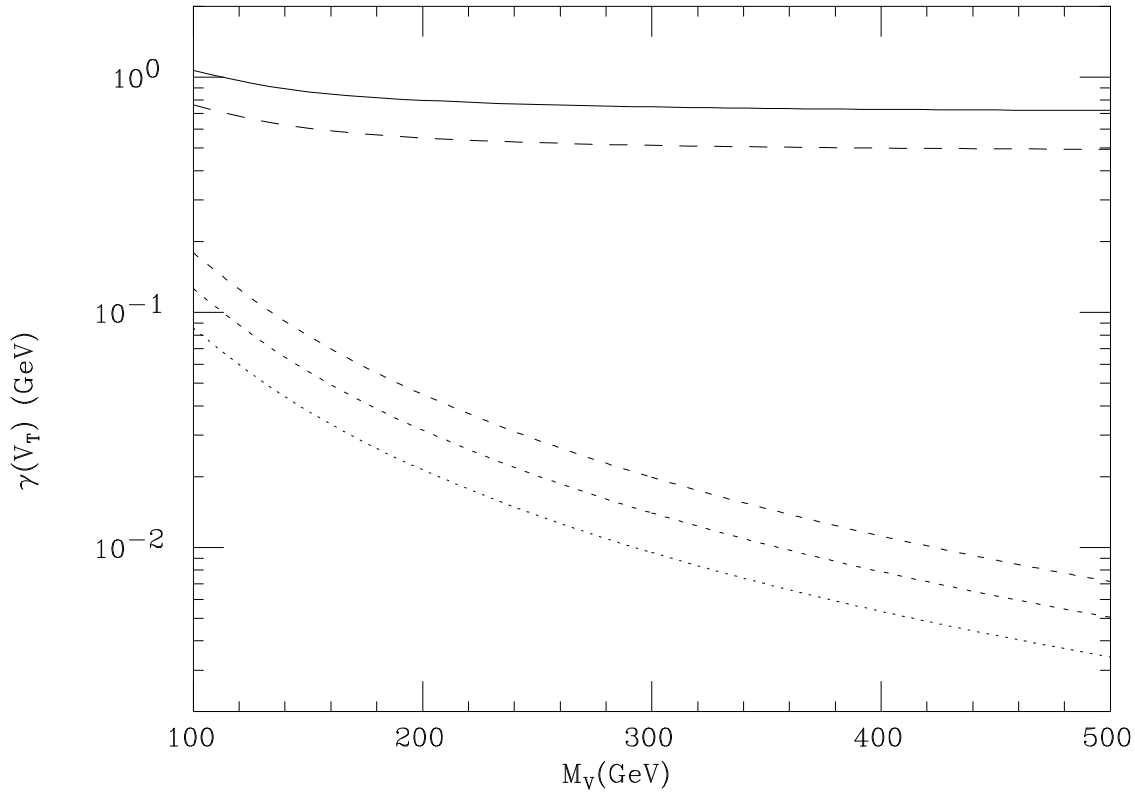


Figure 5: *Decay rates as in Fig. 4, with $Q_U + Q_D = 0$; from Ref. [26].*

rapidly than they do in a walking theory. As mentioned, there must be a tower of ρ_T and ω_T extending up to M_{ETC} . How these affect the spectral integrals that define S is unknown. Another issue that may affect S is that it is usually defined assuming that the new physics appears at energies well above $M_{W,Z}$. We shall see below that, on the contrary, walking technicolor suggests that there are π_T and ρ_T starting near or not far above 100 GeV.

The large value of M_{ETC} makes it difficult if not impossible to explain the top mass by the conventional ETC mechanism, Eq. (2). The most plausible dynamical explanation assumes another gauge interaction that is strong near 1 TeV. This interaction, called topcolor, is like technicolor for the third generation, but it must be more complicated to avoid making $m_b = m_t$. The variant we describe here is called topcolor–assisted technicolor (TC2).

In TC2, as in many top-condensate models of electroweak symmetry breaking, ²¹⁾ almost all of the top quark mass arises from the strong topcolor interaction. ¹⁸⁾ To maintain electroweak symmetry between (left-handed) top and bottom

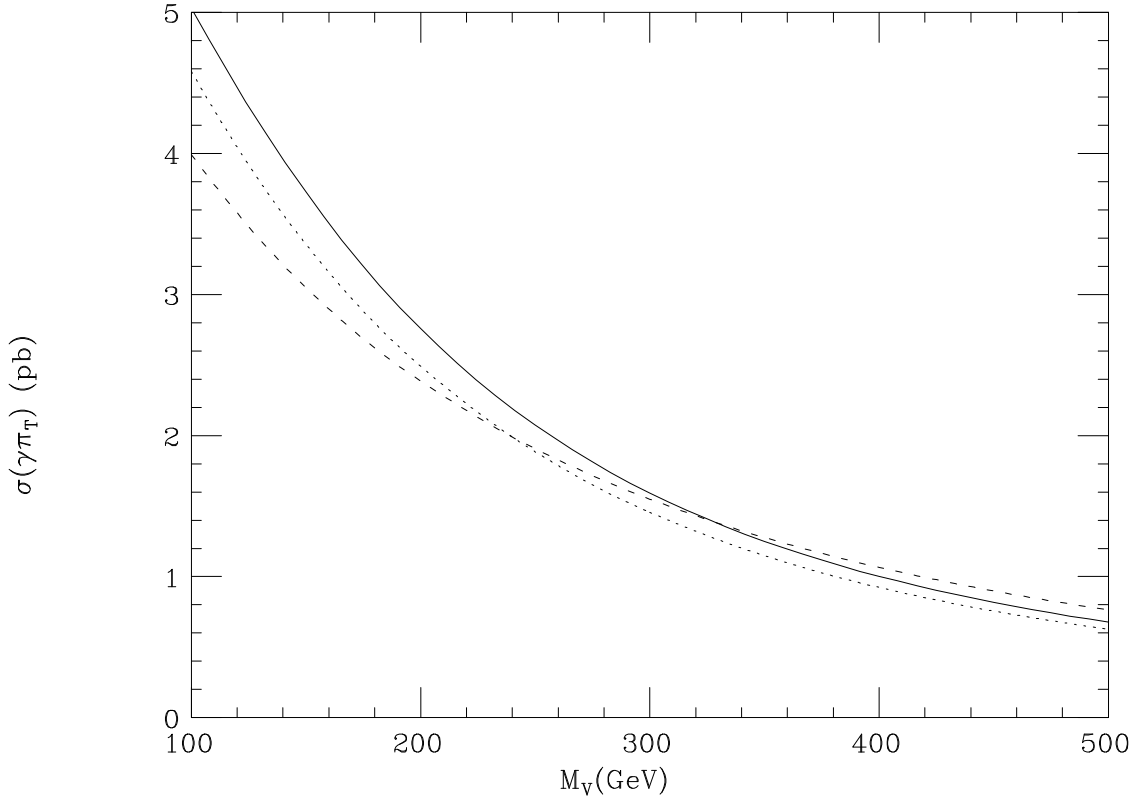


Figure 6: Production rates in $p\bar{p}$ collisions at $\sqrt{s} = 2$ TeV for the sum of ω_T , ρ_T^0 , $\rho_T^\pm \rightarrow \gamma\pi_T$ versus M_V , for $M_{\rho_T} = 210$ GeV and $M_{\omega_T} = 200$ (dotted curve), 210 (solid), and 220 GeV (short-dashed); $Q_U + Q_D = 5/3$, and $M_{\pi_T} = 110$ GeV; from Ref. [26].

quarks and yet not generate $m_b \simeq m_t$, the topcolor gauge group under which (t, b) transform is usually taken to be $SU(3) \otimes U(1)$. The $U(1)$ acts differently on t_R and b_R and, so, provides the difference that causes only top quarks to condense. Then, in order that topcolor interactions be natural—i.e., that their energy scale not be far above m_t —without introducing large weak isospin violation, it is necessary that electroweak symmetry breaking is still mainly due to technicolor interactions.¹⁷⁾ Extended technicolor interactions are still needed in TC2 models to generate the masses of light quarks and the bottom quark, to contribute a few GeV to m_t ,¹ and to give mass to technipions. The scale of ETC interactions still must be hundreds of TeV to suppress flavor-changing neutral currents and, so, the technicolor coupling

¹Massless Goldstone “top-pions” arise from top-quark condensation. This ETC contribution to m_t is needed to give them a mass in the range of 150–250 GeV.

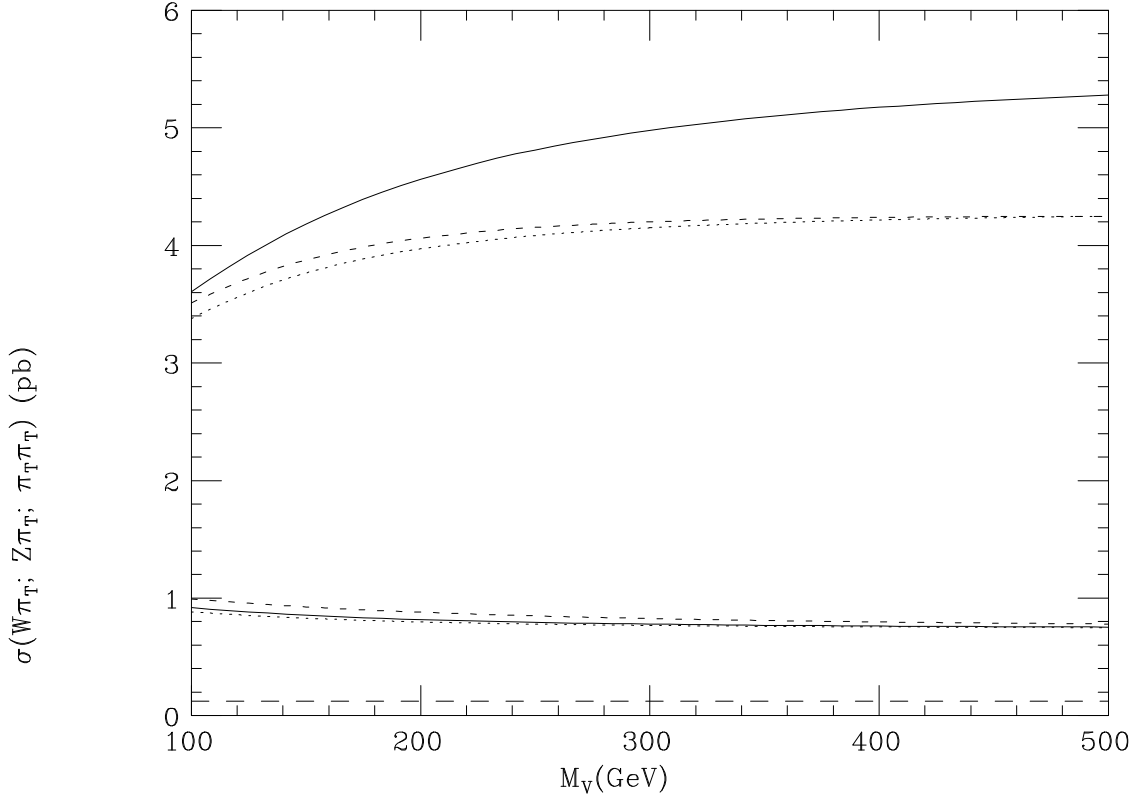


Figure 7: Production rates for $\omega_T, \rho_T^0, \rho_T^\pm \rightarrow W\pi_T$ (upper curves) and $Z\pi_T$ (lower curves) versus M_V , for $M_{\rho_T} = 210$ GeV and $M_{\omega_T} = 200$ (dotted curve), 210 (solid), and 220 GeV (short-dashed); $Q_U + Q_D = 5/3$ and $M_{\pi_T} = 110$ GeV. Also shown is $\sigma(\rho_T \rightarrow \pi_T\pi_T)$ (lowest dashed curve); from Ref. [26].

still must walk.

Walking technicolor requires that the beta-function $\beta(\alpha_{TC})$ be near zero for a large range of energy above Λ_{TC} . This requires many technifermions in the fundamental representation of $SU(N_{TC})$, or a few in higher-dimensional representations, or both. ²²⁾ The TC2 models that are consistent with the pattern of quark masses and the mixings between the heavy and light generations also require many (~ 10) technidoublets. ^{23, 24)}

All this suggests that the technicolor scale is much lower than previously thought. If the number N of technidoublets is $\mathcal{O}(10)$, then $\Lambda_{TC} \simeq F_T = F_\pi/\sqrt{N} \lesssim 100$ GeV. This sets the mass scale for the lightest color-singlet technivector mesons, $M_{\rho_T} \simeq M_{\omega_T} \simeq 2\Lambda_{TC} \lesssim 200$ GeV. The lightest color-octet ρ_T , formed from color-triplet technifermions (which are needed in TC2) will be heavier, starting, perhaps,

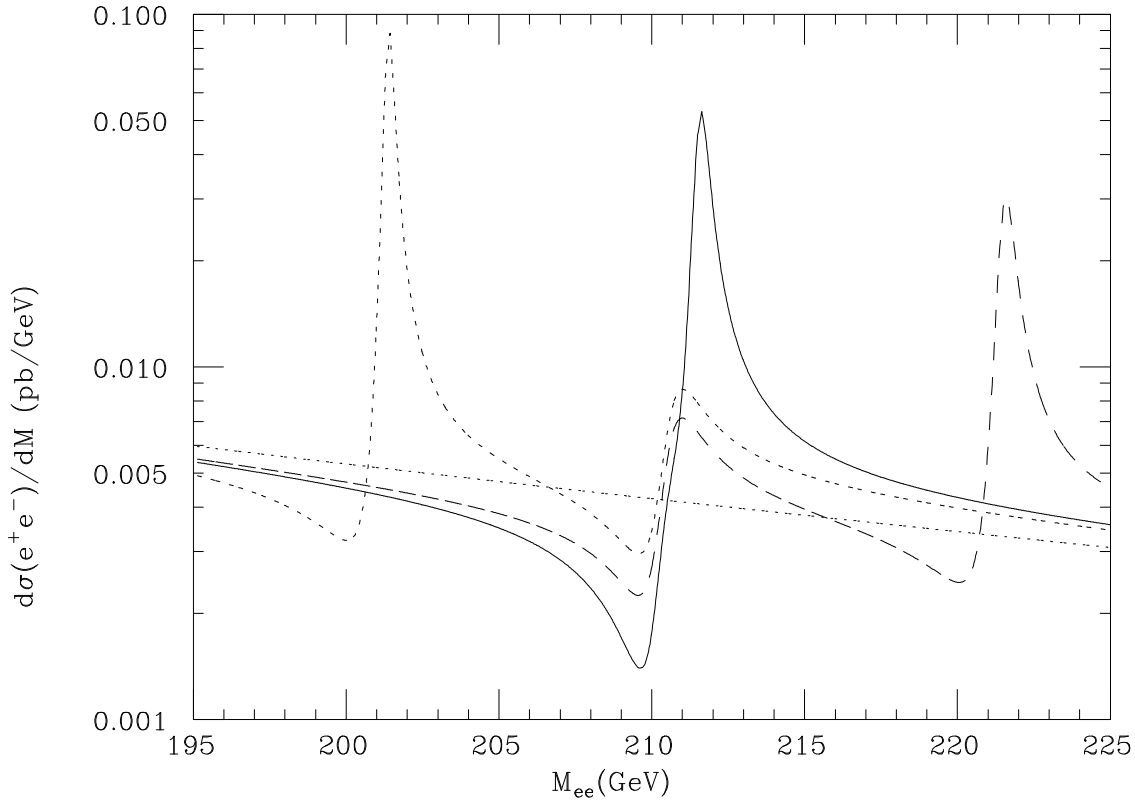


Figure 8: *Invariant mass distributions for $\omega_T, \rho_T^0 \rightarrow e^+e^-$ for $M_{\rho_T} = 210$ GeV and $M_{\omega_T} = 200$ (short-dashed curve), 210 (solid), and 220 GeV (long-dashed); $M_V = 100$ GeV. The standard model background is the sloping dotted line. $Q_U + Q_D = 5/3$ and $M_{\pi_T} = 110$ GeV; from Ref. [26].*

at 400–500 GeV. There are $4N^2 - 4$ technipions in addition to W_L^\pm and Z_L^0 . The color-singlet π_T may have masses as low as 100 GeV. In short, unlike the situation in minimal technicolor, these technihadrons may be within reach of Tevatron Run II. They are certainly accessible at the LHC. Color-singlet ρ_T and ω_T may even be detected at LEP200. If the NLC or a muon collider is built, it will be able carry out precision studies of color-singlet technihadrons. We turn now to the signatures of this “low-scale technicolor” (25, 26, 27):² How are the ρ_T, ω_T , and π_T produced, and how do they decay?

Color-singlet ρ_T and ω_T are produced in the s -channel of $\bar{q}q$ and e^+e^- annihilation. Color-octet ρ_{T8} are produced in $\bar{q}q$ and gg collisions. In QCD-like technicolor, they decay mainly to two or more technipions, with ρ_{T8} decaying to

²Many of these signatures are now encoded in PYTHIA. (28)

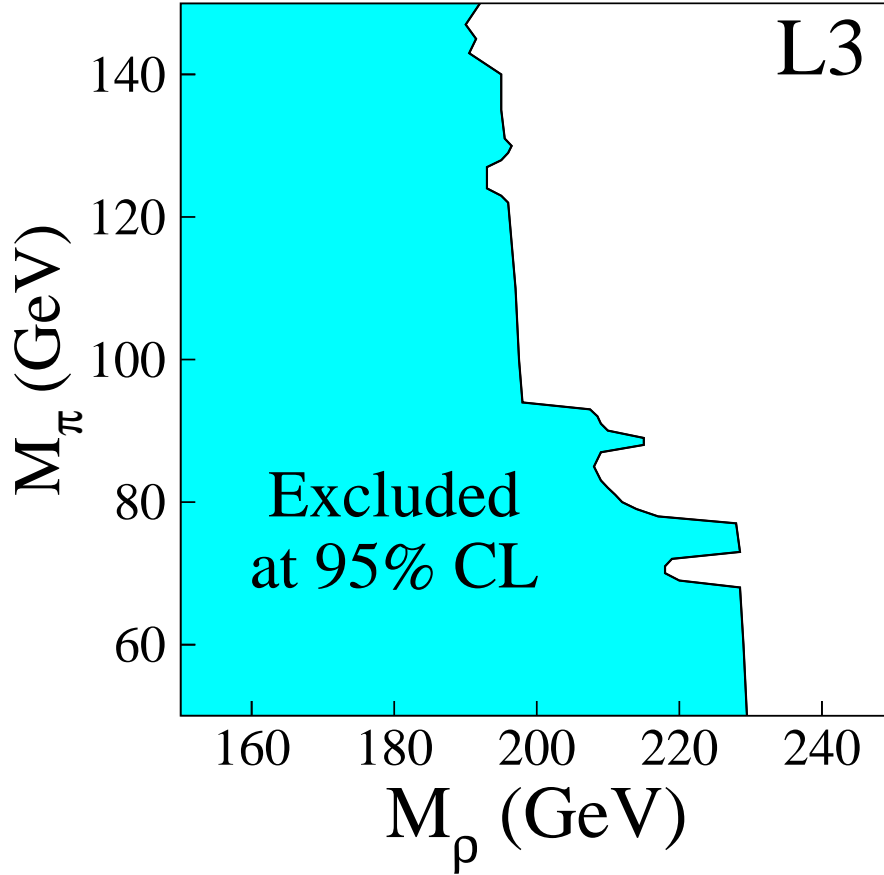


Figure 9: *The M_{ρ_T} - M_{π_T} region excluded by L3 at the 95% CL; from Ref. [30].*

color-octet and color-triplet (leptoquark) pairs. Walking technicolor dramatically changes this expectation.

In the extreme walking limit, $\langle \bar{T}T \rangle_{ETC} \simeq (M_{ETC}/\Lambda_{TC})\langle \bar{T}T \rangle_{TC}$, the technipions have masses of order Λ_{TC} , and they are not pseudoGoldstone bosons at all. Though this extreme limit is theoretically problematic because it is exactly scale-invariant, it is clear that walking TC enhances π_T masses significantly more than it does the ρ_T and ω_T masses. Thus, it is likely that $M_{\pi_T} \gtrsim \frac{1}{2}M_{\rho_T, \omega_T}$ and, so, the nominal isospin-conserving decay channels $\rho_T \rightarrow \pi_T \pi_T$ and $\omega_T \rightarrow \pi_T \pi_T \pi_T$ are *closed*.²²⁾ We discuss our expectations first for the color-singlet sector, then for color-nonsinglets.

Theory and Experiment for Color-Singlet Technihadrons

The flavor problem is hard whether it is attacked with extended technicolor or any other weapon. After all these years nobody has a complete solution or even a

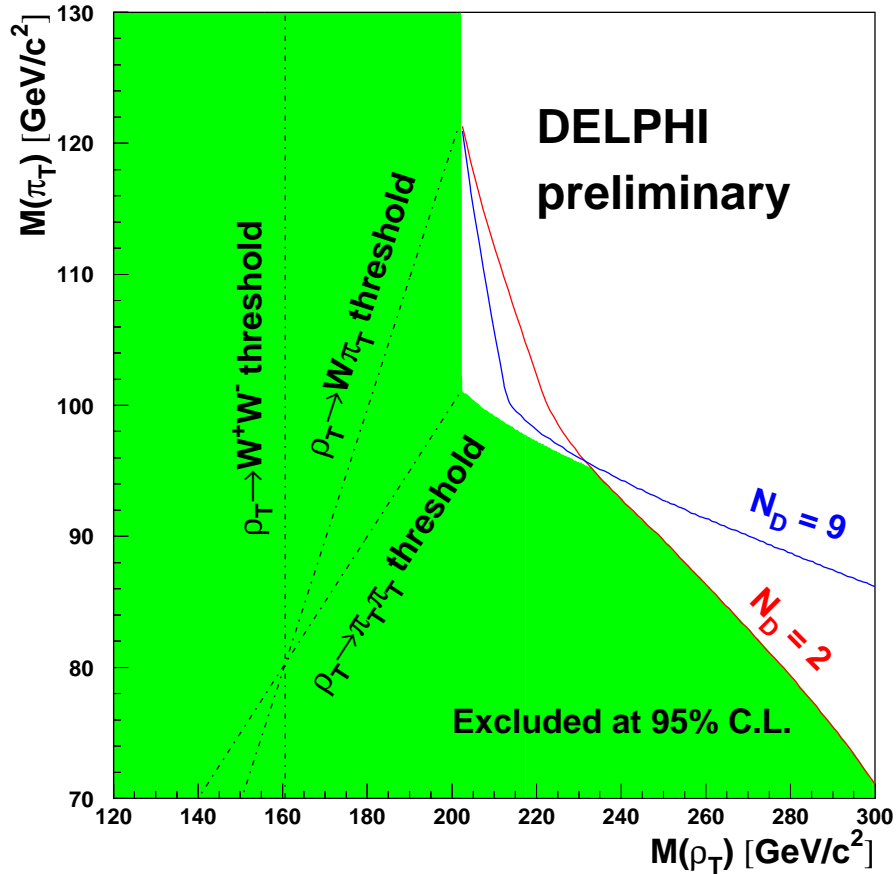


Figure 10: The $M_{\rho_T} - M_{\pi_T}$ region excluded at the 95% CL by the DELPHI analysis of Ref. [31].

promising scenario. In the absence of an explicit ETC model, or any other kind of model, we need experimental guidance. Experimentalists, in turn, need guidance from theorists to constrain their schemes. Supersymmetry has its MSSM. What follows is a description of the corresponding thing for technicolor, in the sense that it defines a set of incisive experimental tests in terms of a limited number of adjustable parameters. I call this the “Technicolor Straw Man” model (or TCSM). First, I’ll outline it in the color-singlet sector.

In the TCSM, we assume that we can consider *in isolation* the lowest-lying bound states of the lightest technifermion doublet, (T_U, T_D) . These technifermions are likely to be color singlets because, otherwise, color- $SU(3)$ interactions would contribute significantly to their hard (or current-algebra) mass.²⁹⁾ We shall assume that they transform according to the fundamental representation of the technicolor gauge group, $SU(N_{TC})$. Their electric charges are Q_U and $Q_D = Q_U - 1$. The

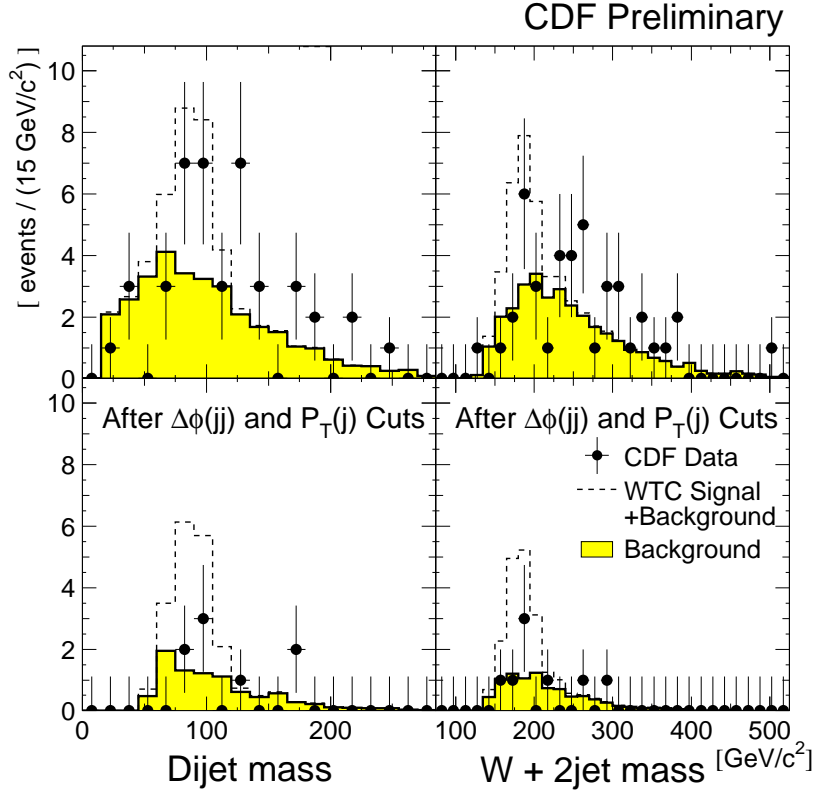


Figure 11: *Invariant mass of the dijet system and of the $W + 2\text{jet}$ system for the $\ell + 2\text{jet}$ mode; from Ref. [32]. The mass combination shown is $M_{\pi_T} = 90\text{ GeV}$ and $M_{\rho_T} = 180\text{ GeV}$.*

bound states in question are vector and pseudoscalar mesons. The vectors include a spin–one isotriplet $\rho_T^{\pm,0}$ and an isosinglet ω_T . In topcolor–assisted technicolor, there is no need to invoke large isospin–violating extended technicolor interactions to explain the top–bottom splitting. Thus, techni–isospin can be, and likely must be, a good approximate symmetry. Then, ρ_T and ω_T will be mostly isovector and isoscalar, respectively, and they will be nearly degenerate. Their production in annihilation processes is described using vector meson dominance and propagator matrices mixing them with W^\pm and γ, Z^0 ; see Ref. [26], called TCSM–1 below. Again, mixing of these ρ_T and ω_T with their excitations is ignored in the TCSM.

The lightest pseudoscalar $\bar{T}T$ bound states, the technipions, also comprise an isotriplet $\Pi_T^{\pm,0}$ and an isosinglet Π_T^0 . However, these are not mass eigenstates; all color–singlet isovector technipions have a W_L component. To limit the number of parameters in the TCSM, we make the simplifying assumption that the isotriplets are simple two–state mixtures of the W_L^\pm, Z_L^0 and the lightest mass–eigenstate pseudo–

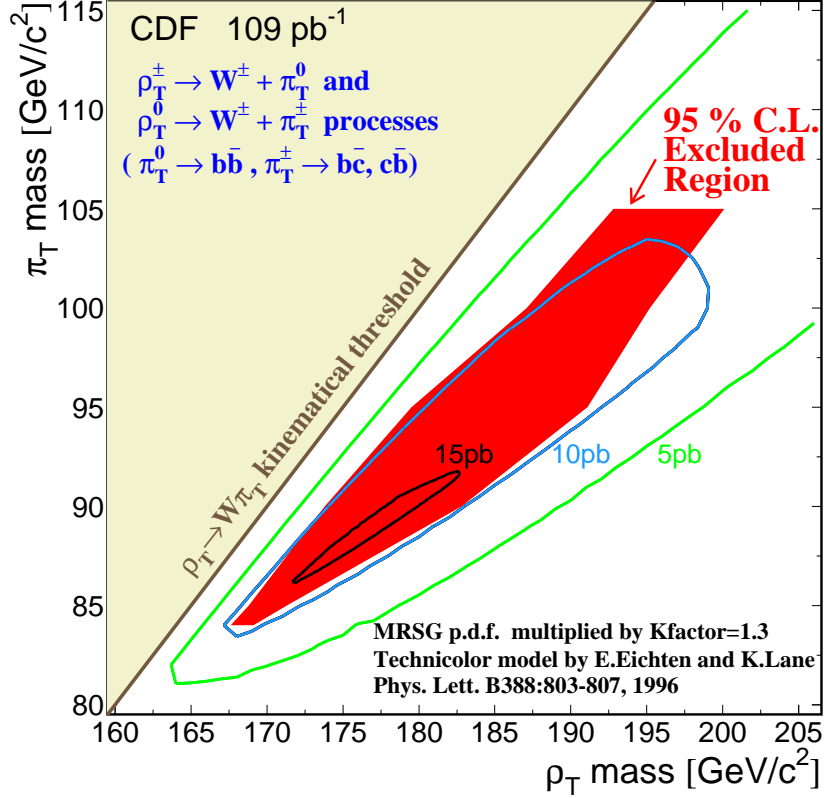


Figure 12: *Excluded region for the CDF search for $\rho_T \rightarrow W^\pm \pi_T$ in Ref. [32]. See that reference for an explanation of the 5, 10, 15 pb contours.*

Goldstone technipions π_T^\pm, π_T^0 :

$$|\Pi_T\rangle = \sin \chi |W_L\rangle + \cos \chi |\pi_T\rangle. \quad (9)$$

Here, $\sin \chi = F_T/F_\pi = 1/\sqrt{N} \ll 1$.

Similarly, $|\Pi_T^0\rangle = \cos \chi' |\pi_T^0\rangle + \dots$, where χ' is another mixing angle and the ellipsis refers to other technipions needed to eliminate the two-technigluon anomaly from the Π_T^0 chiral current. It is unclear whether, like ρ_T^0 and ω_T , the neutral technipions π_T^0 and $\pi_T^{\prime 0}$ will be degenerate as we have previously supposed.²⁵⁾ On one hand, they both contain the lightest $\bar{T}T$ as constituents. On the other, $\pi_T^{\prime 0}$ must contain other, presumably heavier, technifermions as a consequence of anomaly cancellation. We assume that π_T^0 and $\pi_T^{\prime 0}$ are nearly degenerate. If this is true, and if their widths are roughly equal, there will be appreciable π_T^0 - $\pi_T^{\prime 0}$ mixing. Then, the lightest neutral technipions will be ideally-mixed $\bar{T}_U T_U$ and $\bar{T}_D T_D$ bound states. In any case, the technipions, assumed here to be lighter than $m_t + m_b$, are expected to decay as follows: $\pi_T^+ \rightarrow c\bar{b}$ or $c\bar{s}$ or even $\tau^+ \nu_\tau$; $\pi_T^0 \rightarrow b\bar{b}$ and, perhaps $c\bar{c}$, $\tau^+ \tau^-$;

V_T Decay Mode	$V(V_T \rightarrow G\pi_T) \times M_V/e$	$A(V_T \rightarrow G\pi_T) \times M_A/e$
$\omega_T \rightarrow \gamma\pi_T^0$	$\cos \chi$	0
$\rightarrow \gamma\pi_T^{0'}$	$(Q_U + Q_D) \cos \chi'$	0
$\rightarrow Z^0\pi_T^0$	$\cos \chi \cot 2\theta_W$	0
$\rightarrow Z^0\pi_T^{0'}$	$-(Q_U + Q_D) \cos \chi' \tan \theta_W$	0
$\rightarrow W^\pm\pi_T^\mp$	$\cos \chi/(2 \sin \theta_W)$	0
$\rho_T^0 \rightarrow \gamma\pi_T^0$	$(Q_U + Q_D) \cos \chi$	0
$\rightarrow \gamma\pi_T^{0'}$	$\cos \chi'$	0
$\rightarrow Z^0\pi_T^0$	$-(Q_U + Q_D) \cos \chi \tan \theta_W$	0
$\rightarrow Z^0\pi_T^{0'}$	$\cos \chi' \cot 2\theta_W$	0
$\rightarrow W^\pm\pi_T^\mp$	0	$-\cos \chi/(2 \sin \theta_W)$
$\rho_T^\pm \rightarrow \gamma\pi_T^\pm$	$(Q_U + Q_D) \cos \chi$	0
$\rightarrow Z^0\pi_T^\pm$	$-(Q_U + Q_D) \cos \chi \tan \theta_W$	$\cos \chi / \sin 2\theta_W$
$\rightarrow W^\pm\pi_T^0$	0	$\cos \chi/(2 \sin \theta_W)$
$\rightarrow W^\pm\pi_T^{0'}$	$\cos \chi'/(2 \sin \theta_W)$	0

Table 1: *Relative vector and axial vector amplitudes for $V_T \rightarrow G\pi_T$ with $V_T = \rho_T, \omega_T$ and G a transverse electroweak boson, γ, Z^0, W^\pm ; from Ref. [26].*

and $\pi_T^{0'} \rightarrow gg, b\bar{b}, c\bar{c}, \tau^+\tau^-$. This puts a premium on heavy-flavor identification in collider experiments. However, this is only an educated guess and it is possible that the mass-eigenstate neutral π_T have a sizable branching ratio to gluon (or even light-quark) pairs.

For vanishing electroweak couplings g, g' , the ρ_T and ω_T decay as

$$\begin{aligned}
\rho_T &\rightarrow \Pi_T\Pi_T = \cos^2 \chi (\pi_T\pi_T) + 2 \sin \chi \cos \chi (W_L\pi_T) + \sin^2 \chi (W_LW_L); \\
\omega_T &\rightarrow \Pi_T\Pi_T\Pi_T = \cos^3 \chi (\pi_T\pi_T\pi_T) + \dots .
\end{aligned} \tag{10}$$

As noted above however, the all- π_T modes are likely to be closed. Thus, major decay modes of the ρ_T will be $W_L\pi_T$ or, if $M_{\rho_T} \lesssim 180$ GeV (a possibility we regard as unlikely, if not already eliminated by LEP data), W_LW_L . The $W_L^\pm\pi_T^{\mp,0}$ and $Z_L^0\pi_T^\pm$ decays of ρ_T have striking signatures in any collider. Only at LEP is it now possible to detect $\rho_T^0 \rightarrow W^+W^-$ above background. If $M_{\omega_T} < 250$ GeV, all the $\omega_T \rightarrow \Pi_T\Pi_T\Pi_T$ modes are closed. In all cases, the ρ_T and ω_T are very narrow, $\Gamma(\omega_T) \lesssim \Gamma(\rho_T) \lesssim 1$ GeV, because of the smallness of $\sin \chi$ and the limited phase space. Therefore, we must consider other decay modes. These are electroweak, suppressed by powers of α , but not by phase space.

The decays $\rho_T, \omega_T \rightarrow G\pi_T$, where G is a transversely polarized electroweak gauge boson, and $\rho_T, \omega_T \rightarrow \bar{f}f$ were calculated in TCSM-1. The $G\pi_T$ modes have rates of $\mathcal{O}(\alpha)$, while the fermion mode $\bar{f}f$ rates are $\mathcal{O}(\alpha^2)$. The $\Gamma(\rho_T, \omega_T \rightarrow G\pi_T)$

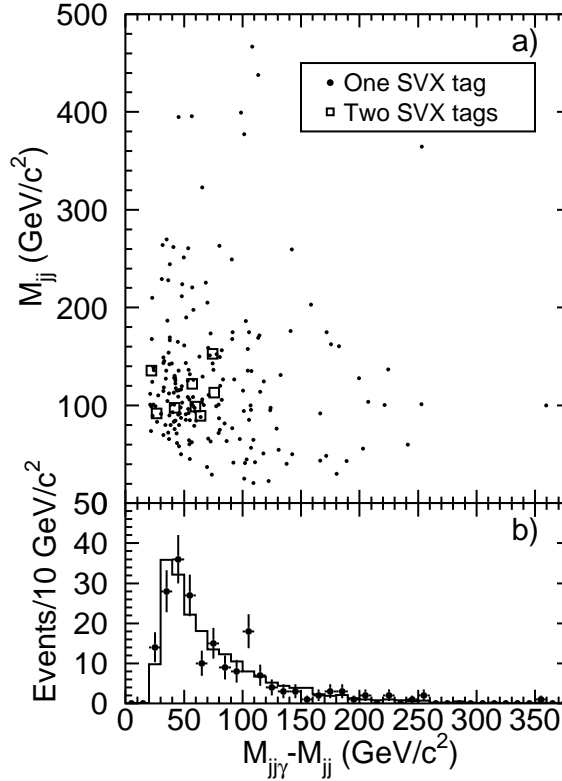


Figure 13: (a) The distribution of M_{jj} vs. $M_{jj\gamma} - M_{jj}$ for events with a photon, b -tagged jet and a second jet. (b) Projection of this data in $M_{jj\gamma} - M_{jj}$; from Ref. [33]

are suppressed by $1/M_V^2$ or $1/M_A^2$, depending on whether the vector or axial vector part of the electroweak current is involved in the decay. Here, $M_{V,A}$ are masses of order Λ_{TC} occurring in the dimension-5 operators for these decays. We usually take them equal and vary them from 100 to 400 GeV. For smaller values of $M_{V,A}$, these modes, especially the $\gamma\pi_T$ ones, are as important as the $W_L\pi_T$ modes. For larger $M_{V,A}$ and $|Q_U + Q_D| \gtrsim 1$, the $\bar{f}f$ decay modes may become competitive. Table 1 lists the relative strengths of the decay amplitudes for the $\rho_T, \omega_T \rightarrow G\pi_T$ processes. Figure 4 gives a sense of the $M_{V,A}$ dependence of the total decay rates of ρ_T and ω_T for $M_{\rho_T} = 210$ GeV, $M_{\omega_T} = 200\text{--}220$ GeV, $M_{\pi_T} = 110$ GeV, and $Q_U = Q_D + 1 = 4/3$. Figure 5 shows the rates for $Q_U = -Q_D = 1/2$. These and all subsequent calculations assume that $N_{TC} = 4$ and $\sin \chi = \sin \chi' = 1/3$. Experimental analyses quoted below use the same defaults and (usually) $Q_U = Q_D + 1 = 4/3$.

Figures 6 and 7 show the cross sections in $\bar{p}p$ collisions at $\sqrt{s} = 2$ TeV for production of $\gamma\pi_T$ and for $W\pi_T, Z\pi_T$ and $\pi_T\pi_T$ as a function of $M_V = M_A$. Figure 8

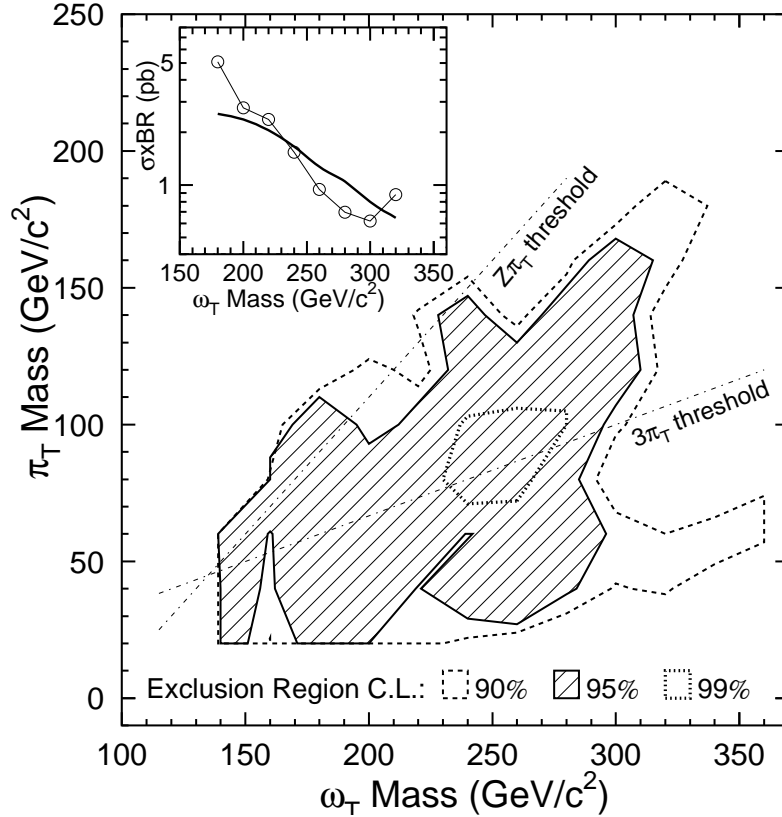


Figure 14: The 90%, 95% and 99% CL exclusion regions for the CDF search for $\omega_T \rightarrow \gamma\pi_T$ in Ref. [33]. The inset shows the limit on σB for $M_{\pi_T} = 120$ GeV. The circles represent the limit and the solid line the prediction from the second paper in Ref. [25].

shows the e^+e^- rate for $M_V = 100$ GeV. ²⁶⁾ In these three graphs, $Q_U = Q_D + 1 = 4/3$. The production rates in these figures, all in the picobarn range, are typical for the Tevatron for $M_{\rho_T, \omega_T} \lesssim 250$ GeV and $M_{\pi_T} \lesssim 150$ GeV. Thus, Run II will probe a significant portion of low-scale technicolor parameter space.

Turning to the recent searches for color-singlet technihadrons, we start with a study by the L3 Collaboration at LEP. ³⁰⁾ This search is based on 176 pb^{-1} of data taken at an average energy of 189 GeV. The L3 analysis used TCSM-1 and it studied the channels $e^+e^- \rightarrow \rho_T^0 \rightarrow W^+W^-$; $W_L^\pm \pi_T^\mp \rightarrow \ell \nu_\ell bc$; $\pi_T^+ \pi_T^- \rightarrow c\bar{b}b\bar{c}$; and $\gamma\pi_T^0 \rightarrow \gamma b\bar{b}$. The TC-scale masses were fixed at $M_V = M_A = 200$ GeV and the technifermion charges ranged over $Q_U + Q_D = 5/3, 0, -1$. The resulting 95% confidence limits in the $M_{\rho_T} - M_{\pi_T}$ plane are shown in Fig. 9. A similar study was also carried out by the DELPHI Collaboration ³¹⁾ and its exclusion plot is shown

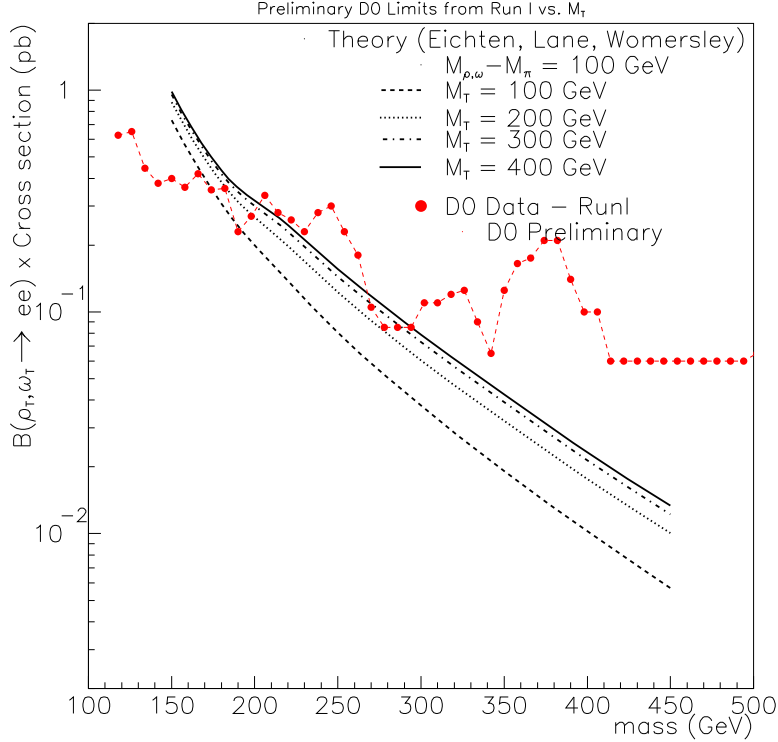


Figure 15: *Excluded regions for the $D\bar{O}$ search for $\rho_T^0, \omega_T \rightarrow e^+e^-$; from Ref. [34].*

in Fig. 10. Note that LEP experiments can be sensitive to ρ_T masses significantly above the e^+e^- cm energy, \sqrt{s} . This is because the e^+e^- cross section on resonance is very large for the narrow ρ_T .

Since these LEP analyses were done, I have realized the cross section formulae stated in TCSM-1 are inappropriate for \sqrt{s} well below M_{ρ_T} . This is unimportant for the Tevatron and LHC, where the production rate comes mainly from integrating over the resonance pole. However, it may have a significant effect on limits derived from e^+e^- annihilation. This is especially true for the W^+W^- channel, which has a large standard model amplitude interfering with the TCSM one.³ Another example is that limits on M_{π_T} approaching $\sqrt{s}/2$ should be derivable from $e^+e^- \rightarrow \pi_T^+\pi_T^-$.

The CDF Collaboration has analyzed Tevatron Run I data to search for the processes signalled by a W or photon plus two jets, one of which is b -tagged:

$$\begin{aligned}
 \bar{q}q \rightarrow W^\pm, \gamma, Z^0 &\rightarrow \rho_T^\pm \rightarrow W_L^\pm \pi_T \rightarrow \ell^\pm \nu_\ell b + \text{jet} \\
 &\rightarrow \rho_T^\pm, \rho_T^0, \omega_T \rightarrow \gamma \pi_T \rightarrow \gamma b + \text{jet}.
 \end{aligned} \tag{11}$$

³I thank F. Richard for drawing my attention to this shortcoming of TCSM-1. A correction will be issued soon.

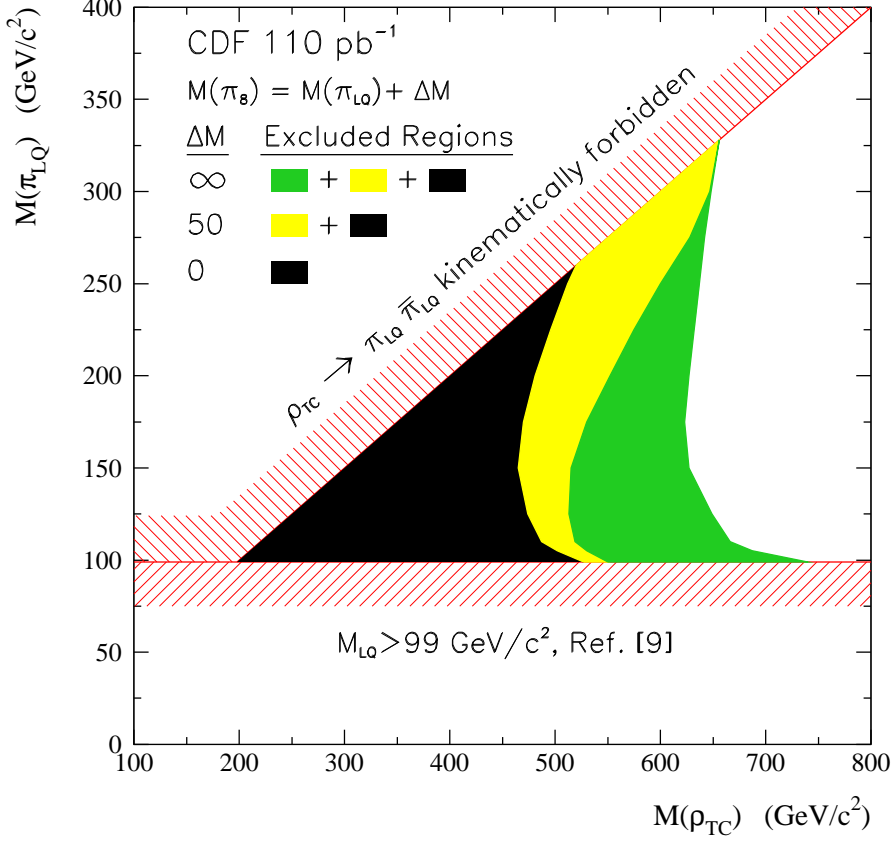


Figure 16: The 95% CL exclusion regions for various $M_{\pi_{T8}} - M_{\pi_{LQ}}$ from a CDF search for $\rho_{T8} \rightarrow \pi_{LQ}\pi_{QL} \rightarrow \tau^+\tau^- \text{jet jet}$; from Ref. [36].

These analyses were carried out before the publication of TCSM-1 so they do not include the $G\pi_T$ and $\bar{f}f$ processes and corresponding branching ratios. They will be included in analyses of Run II data. Figure 11 shows data for the $W\pi_T$ search on top of a background and signal expected for default parameters with $M_{\rho_T} = 180 \text{ GeV}$ and $M_{\pi_T} = 90 \text{ GeV}$. The topological cuts leading to the lower figure are described in the second paper of Ref. [25]. The region excluded at 95% confidence level is shown in Fig. 12. ³²⁾

Figure 13 shows the invariant mass of the tagged and untagged jets and the invariant mass difference $M(\gamma+b+\text{jet}) - M(b+\text{jet})$ in a search for $\omega_T, \rho_T \rightarrow \gamma\pi_T$. ³³⁾ The good resolution in this mass difference is controlled mainly by that of the electromagnetic energy. The exclusion plot is shown in Fig. 14. It is amusing that the $\sim 2\sigma$ excesses in Figs. 11 and 13 correspond to nearly the same $M_{\rho_T, \omega_T} \simeq 200 \text{ GeV}$ and $M_{\pi_T} \simeq 100 \text{ GeV}$.

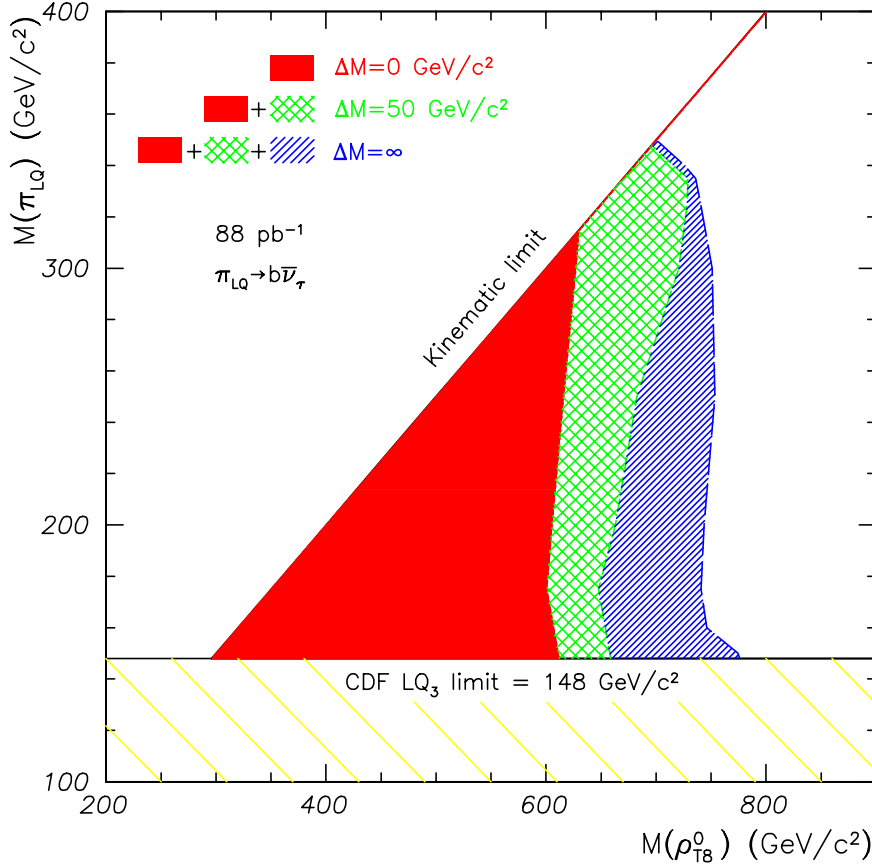


Figure 17: The 95% CL exclusion regions for various $M_{\pi_{T8}} - M_{\pi_{LQ}}$ from a CDF search for $\rho_{T8} \rightarrow \pi_{LQ}\pi_{\bar{Q}L} \rightarrow \bar{b}b\nu\nu$; from Ref. [37].

The DØ Collaboration has studied its Run I Drell–Yan data to search for $\rho_T, \omega_T \rightarrow e^+e^-$.³⁴⁾ The data and the excluded region are shown in Fig. 15 for $Q_U = Q_D + 1 = 4/3$, $M_V = 100\text{--}400$ GeV and $M_{\rho_T} - M_{\pi_T} = 100$ GeV. Increasing M_V (called M_T in the figure) and decreasing $M_{\rho_T} - M_{\pi_T}$ both increase the branching ratio for the e^+e^- channel, the former because it decreases $\rho_T, \omega_T \rightarrow \gamma\pi_T$, the latter because it decreases $\rho_T \rightarrow W\pi_T$. For the parameters considered here, $M_{\rho_T} = M_{\omega_T} < 150\text{--}200$ GeV is excluded at the 95% CL.

Color–Nonsinglet Technihadrons

We turn now to the color–nonsinglet sector. So far, most of the experimental searches have been inspired by the phenomenology of a pre–TCSM, one–family TC model containing a single doublet each of color–triplet techniquarks $Q = (U, D)$ and of color–singlet technileptons $L = (N, E)$.^{35, 9, 29)} Therefore, we defer the details of

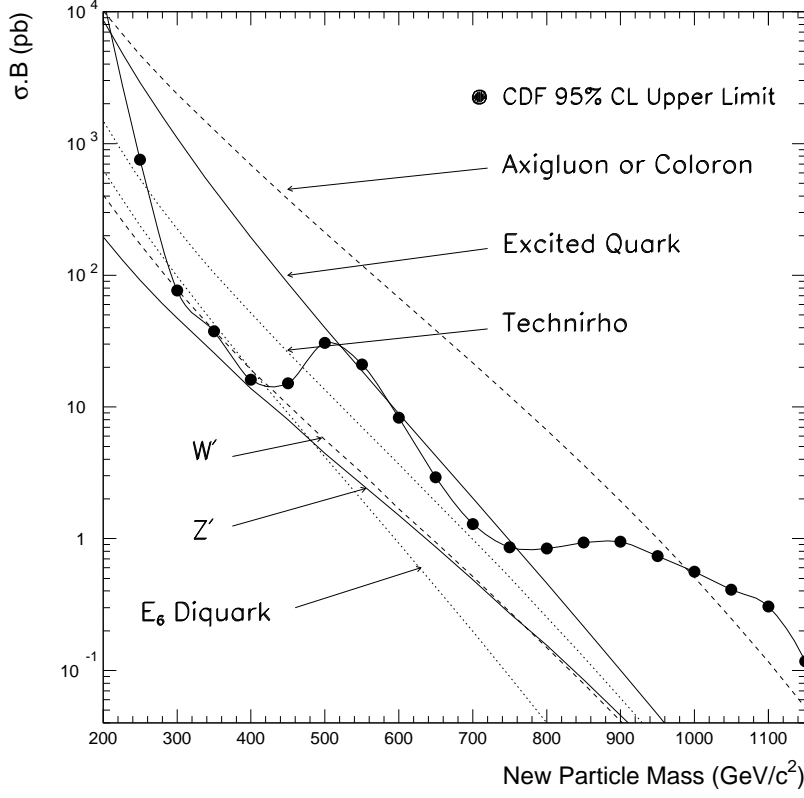


Figure 18: *The 95% exclusions for a CDF search for $\rho_{T8} \rightarrow \text{jet jet}$ and other narrow dijet resonances; from Ref. [38].*

the TCSM for the color–nonsinglet sector to the next section. Assuming that techni–isospin is conserved, production of color–nonsinglet states is assumed to proceed through the lightest isoscalar color–octet technirho, ρ_{T8} :

$$\begin{aligned}
 \bar{q}q, gg \rightarrow g \rightarrow \rho_{T8} &\rightarrow \pi_{T8}\pi_{T8} \\
 &\rightarrow \pi_{LQ}\pi_{\bar{Q}L} \\
 &\rightarrow \bar{q}q, gg \text{ jets} .
 \end{aligned}
 \tag{12}$$

Here, $\pi_{T8} = \pi_{T8}^{\pm}, \pi_{T8}^0, \pi_{T8}^{0'} \equiv \eta_T$ are four color–octet technipions that are expected to decay to heavy $\bar{q}q$ pairs; π_{LQ} are four color–triplet “leptoquarks” expected to decay to heavy $\bar{\ell}q$ with the corresponding charges. If TC2 is invoked, the neutral π_{T8} decay to $\bar{b}b$ and, possibly, gg as readily as to $\bar{t}t$.

The only $\rho_{T8} \rightarrow \pi_T\pi_T$ searches so far are by CDF for leptoquarks $\pi_{ED} \rightarrow \tau^+b$ where the b is not tagged ³⁶⁾ and for $\pi_{ND} \rightarrow \nu b, \nu c$. ³⁷⁾ These are based on 110 pb^{-1} and 88 pb^{-1} of Run I data, respectively. The exclusion plot for the $\tau^+\tau^-$ dijet signal is shown in Fig. 16 as a function of the $\pi_{T8}-\pi_{LQ}$ mass difference.

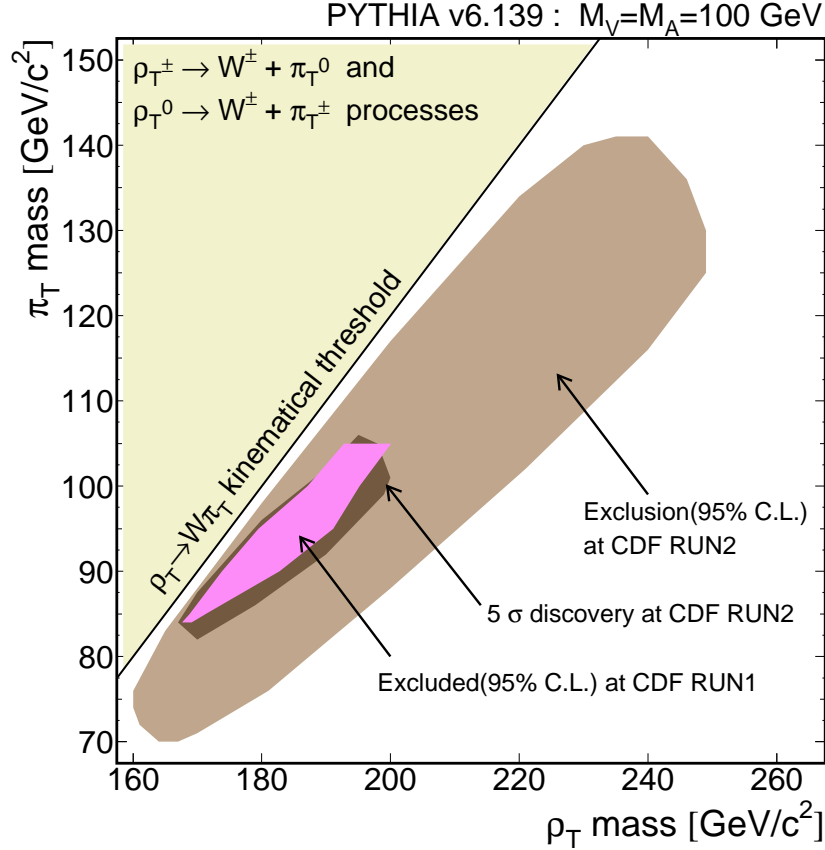


Figure 19: Reach of the CDF detector in Tevatron Run IIa for $\rho_T \rightarrow W^\pm \pi_T$ with $M_V = M_A = 100$ GeV; from Ref. [39].

The theoretically likely case is that this mass difference is about 50 GeV, implying a 95% excluded region extending over $200 \lesssim M_{\rho_{T8}} \simeq 2M_{\pi_{LQ}} \lesssim 500$ GeV. Figure 17 shows the reach for $\rho_{T8}^0 \rightarrow b\bar{b}\nu\bar{\nu}$ with at least one b -jet tagged. Here the 95% limits extends over $300 \lesssim M_{\rho_{T8}} \simeq 2M_{\pi_{LQ}} \lesssim 600$ GeV. The search for $\pi_{LQ} \rightarrow c\nu$ excludes a similar range. These limits are quite impressive. However, it is not clear that they will remain so when complications of TC2 are taken into account in the color-nonsinglet sector. These will be discussed in the next section.

Given the walking technicolor enhancement of π_T masses, it is likely that the $\rho_{T8} \rightarrow \pi_T \pi_T$ channels are closed. In that case, one seeks $\rho_{T8} \rightarrow \text{jet jet}$ in b -tagged and untagged jets. The results of a CDF search for narrow dijet resonances in Run I is shown in Fig. 18. ³⁸⁾ The region $260 < M_{\rho_{T8}} < 460$ GeV is excluded at the 95% confidence level. This, too, is a stringent constraint, but its applicability to TC2 models is uncertain.

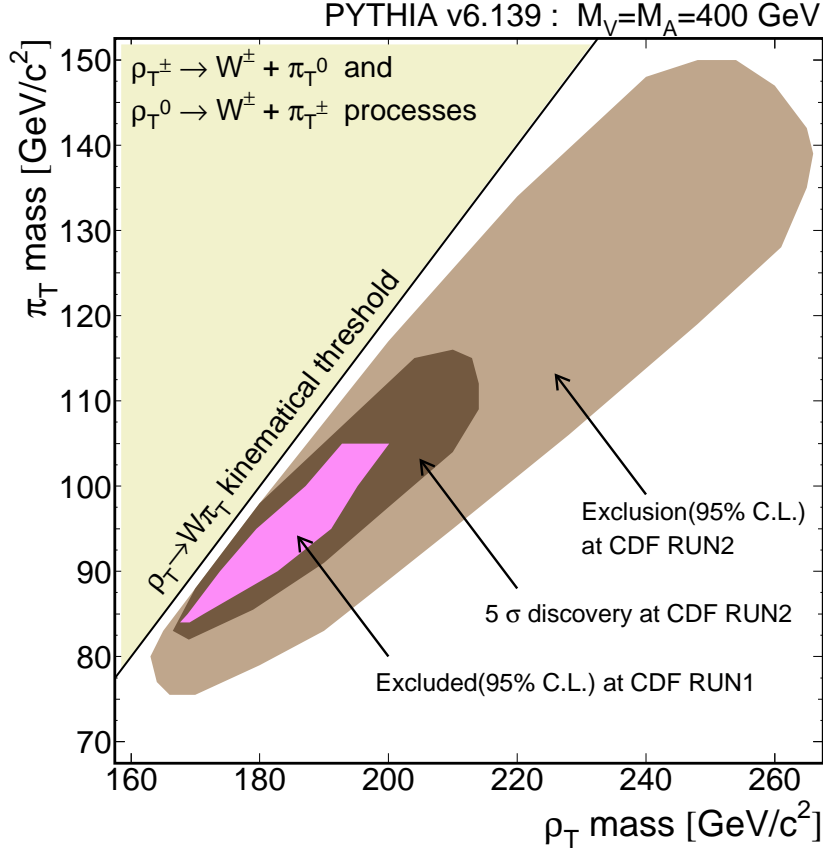


Figure 20: Reach of the CDF detector in Tevatron Run IIa for $\rho_T \rightarrow W^\pm \pi_T$ with $M_V = M_A = 400$ GeV; from Ref. [39].

4. Tomorrow

Run II of the Tevatron Collider begins in Spring 2001. The first stage, Run IIa, is intended to collect 2 fb^{-1} of data with significantly enhanced CDF and $D\bar{O}$ detectors featuring new silicon tracking systems. It is planned that, after a brief shutdown to replace damaged silicon, Run IIb will bring the total data sets for each detector to 15 fb^{-1} or more before the LHC is in full swing in 2006 or so. Low-scale technicolor, if it exists, will be discovered at one of these colliders—most likely the Tevatron!

Studies of the reach for low-scale technicolor using all the processes of the TCSM are just beginning. Early examples do not include sophisticated detector simulations coupled to the event generators. 26, 27, 28) I discuss results for the color-singlet sector first.

The expected reach of CDF in Run IIa for the $\rho_T \rightarrow W^\pm \pi_T \rightarrow \ell^\pm \nu_\ell b \text{ jet}$ processes is shown in Figs. 19 and 20 for the extreme cases $M_V = M_A = 100$ and

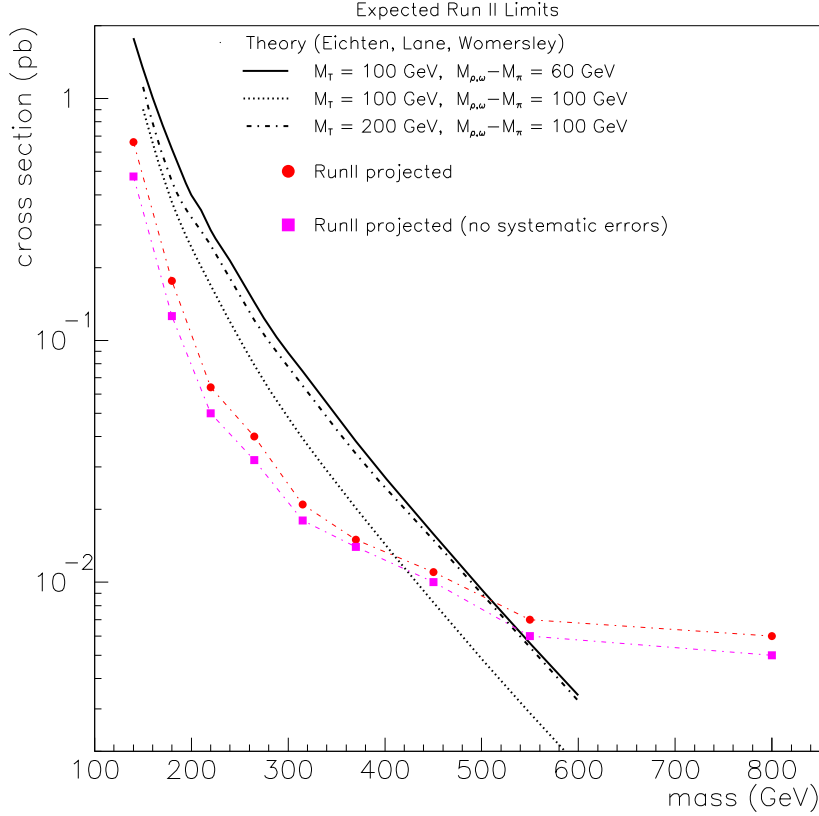


Figure 21: Reach of the $D\bar{O}$ detector in Tevatron Run IIa for $\rho_T^0, \omega_T \rightarrow e^+e^-$; from Ref. [40].

400 GeV. ³⁹⁾ These plots assume the same selections and systematic uncertainty as in the published Run I data, ³²⁾ but double the signal efficiency (1.38% vs. 0.69%). In the case of $M_V = M_A = 100 \text{ GeV}$, the 5σ discovery reach is the same as the 95% excluded region in Run I, while the Run IIa excluded region extends up to $M_{\rho_T} = 240 \text{ GeV}$ and $M_{\pi_T} = 135 \text{ GeV}$. When $M_V = 400 \text{ GeV}$, the 5σ discovery region extends up to $(M_{\rho_T}, M_{\pi_T}) = (210, 115) \text{ GeV}$ while the excluded region reaches to $(260, 145) \text{ GeV}$.

The reach in $\rho_T, \omega_T \rightarrow e^+e^-$ expected by $D\bar{O}$ for $M_V = 100$ and 200 GeV and other TCSM parameters (see above) is shown in Fig. 21. ⁴⁰⁾ Recall that the sensitivity to this process increases as M_V does. As long as $Q_U + Q_D = \mathcal{O}(1)$, masses M_{ρ_T, ω_T} up to 450–500 GeV should be accessible in the e^+e^- channel.

The ATLAS Collaboration has studied its reach for $\rho_T \rightarrow W^\pm Z, W^\pm \pi_T, Z \pi_T$ and for $\omega_T \rightarrow \gamma \pi_T$. ⁴¹⁾ Figure. 22 shows $\rho_T^\pm \rightarrow W^\pm Z \rightarrow \ell^\pm \nu_\ell \ell^+ \ell^-$ for several ρ_T and π_T masses and a luminosity of 10 fb^{-1} . Detailed studies have not been published for this and other modes in which the other TCSM parameters are varied. Still, it

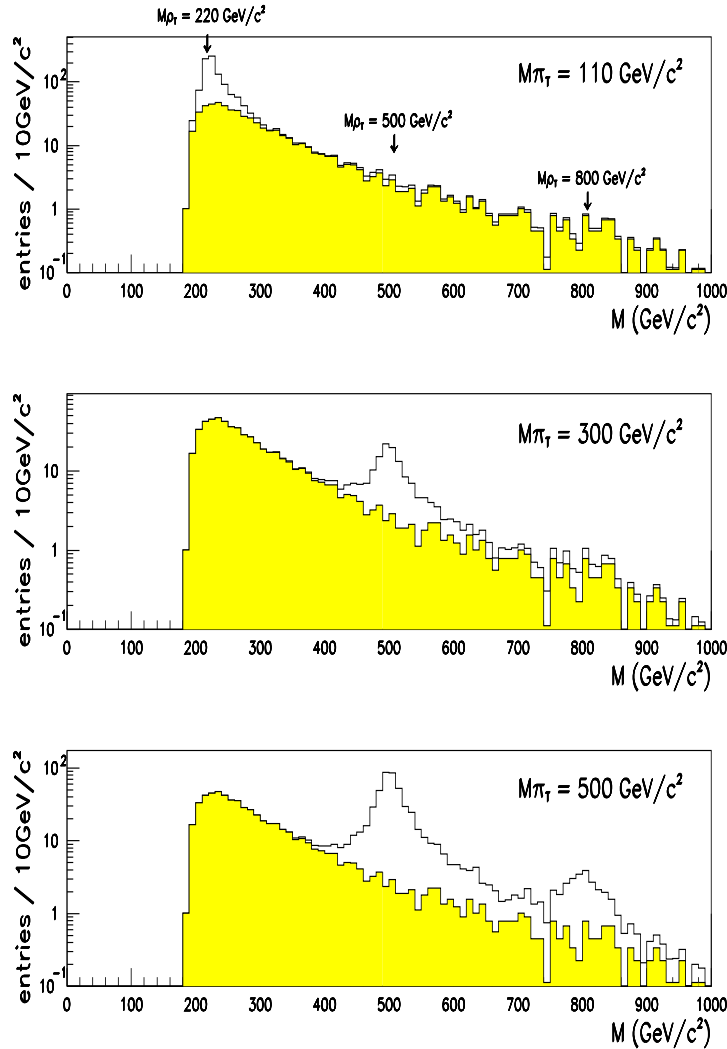


Figure 22: Simulated event and background rates in the ATLAS detector for $\rho_T^\pm \rightarrow W^\pm Z \rightarrow \ell^\pm \nu_\ell \ell^+ \ell^-$ for various M_{ρ_T} and M_{π_T} ; from Ref. [41].

is clear from Fig. 22 that the higher energy and luminosity of the LHC ought to make it possible to completely exclude, or discover, low-scale technicolor for any reasonable set of TCSM parameters.

Finally, and very briefly, I turn to the prospects for studying the color-singlet sector of low-scale technicolor at the Tevatron and LHC; see Ref. [27] (TCSM-2). As I mentioned, the simplest implementation of TC2 models requires two color $SU(3)$ groups, one that is strongly-coupled at 1 TeV for the third generation quarks (t, b) and one that is weakly-coupled for the two light generations. These two color groups must be broken down to the diagonal $SU(3)$ near 1 TeV, and this remaining symmetry is identified with ordinary color. The most economi-

TC2 assisted Strawman TC

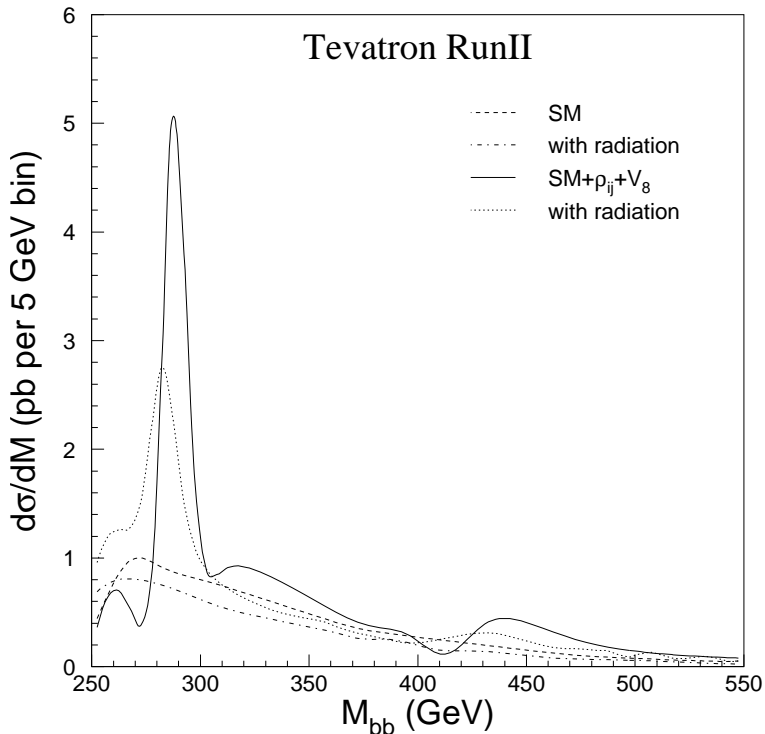


Figure 23: Production of $\bar{b}b$ in $\bar{p}p$ collisions at $\sqrt{s} = 2$ TeV according to the TCSM model of Ref. [27].

cal way to achieve this is to have two doublets of technifermions $T_1 = (U_1, D_1)$ and $T_2 = (U_2, D_2)$, which transform respectively as $(3, 1, N_{TC})$ and $(1, 3, N_{TC})$ under the two color groups and technicolor. They condense with each other to achieve the desired breaking to $SU(3)_C$.²⁴⁾

The main phenomenological consequence of this scenario for TC2 breaking is that the $SU(3)$ gluons mix with an octet of massive “colorons”, V_8^A ($A = 1, \dots, 8$), the gauge bosons of the broken topcolor $SU(3)$, and with four color–octet technirhos $\rho_{ij}^A \sim \bar{T}_i \lambda_A T_j$ ($i, j = 1, 2$).²⁷⁾ The colorons decay strongly to top and bottom quarks and weakly to the light quarks¹⁷⁾. Alternatively, there is a flavor–universal variant of TC2⁴²⁾ in which colorons decay with equal strength to all quark flavors. In TCSM–2, we assume for simplicity that all ρ_{ij} are too light to decay to pairs of technipions.⁴⁾ Then, they decay (via gluon and coloron dominance) into $\bar{q}q$ and gg dijets and into $g\pi_{T8}$ and $g\pi_{T1}$.

⁴⁾The colored technipion sector of a TC2 model is bound to be very rich. Thus, it is not clear how the limits on leptoquarks discussed above are to be interpreted. This is work for the future.

TC2 assisted Strawman TC

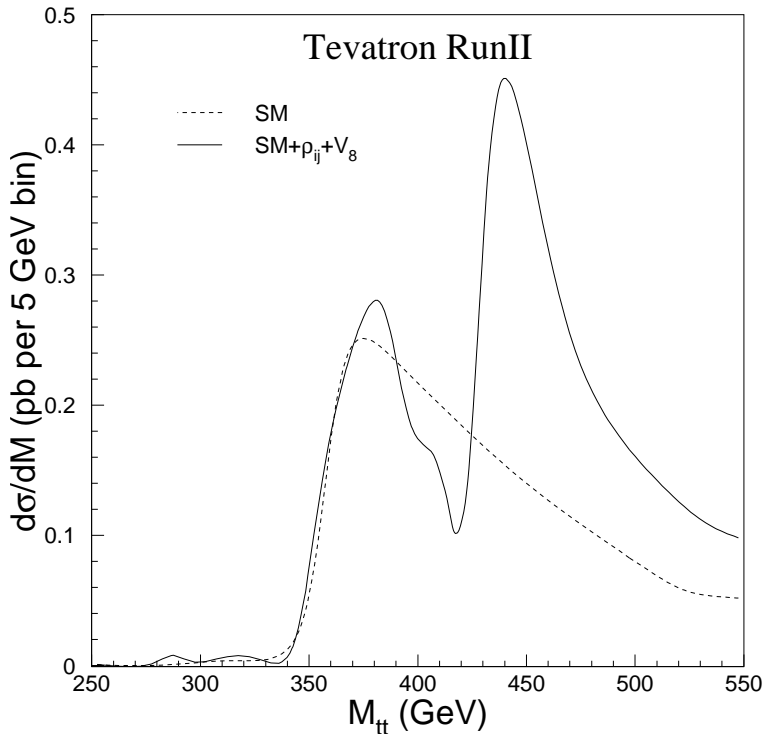


Figure 24: Production of $\bar{t}t$ in $\bar{p}p$ collisions at $\sqrt{s} = 2$ TeV according to the TCSM model of Ref. [27].

Even this minimal, simplified TC2 version of the TCSM has a much richer set of dijet spectra and other hadron collider signals than the one-family model discussed above. (29, 38). We are just beginning to study it. Some preliminary examples of dijet production based on the assumptions of TCSM-2 are shown in Figs. 23 and 24 for $\sqrt{s} = 2$ TeV at the Tevatron. In both figures the coloron mass is 1.2 TeV while the input ρ_{T8} masses range from 350 to 500 GeV.⁵ Figure 23 shows $\bar{b}b$ production with a strong resonance at 300 GeV (i.e., below $\bar{t}t$ threshold). Figure 24 shows $\bar{t}t$ production with roughly a factor of two enhancement over the standard model. Both signals are ruled out by Run I measurements of the $\bar{b}b$ and $\bar{t}t$ cross sections.

Many more studies of both the color-singlet and nonsinglet sectors of the TCSM need to be carried out. An ongoing Run II workshop studying strong dynamics at Fermilab will begin this before Run II starts next March. Presumably, the CDF and DØ collaborations will carry out detector-specific simulations in the next

⁵The pole masses are shifted somewhat from these input values by mixing effects.

year or two. Meanwhile, we can expect more detailed, and more incisive, studies from the LEP collaborations to appear. And we hope that ATLAS and CMS will consider more thoroughly the possibility of strong dynamics beyond the standard model before they begin their runs later in the decade.

Acknowledgements

I wish to express my appreciation for a very stimulating conference at La Thuile 2000 to the organizers Giorgio Belletini, Mario Greco, Giorgio Chiarelli and to Claudia Tofani and other members of the marvelous secretariat. I am indebted to my colleagues, members of the Run II Strong Dynamics Workshop and others for their help and constructive comments throughout the course of this work. In particular, I thank Georges Azuelos, Sekhar Chivukula, Estia Eichten, Andre Kounine, Greg Landsberg, Richard Haas, Takanobu Handa, Robert Harris, Kaori Maeshima, Meenakshi Narain, Steve Mrenna, Steve Parke, Francois Richard, Elizabeth Simmons, and John Womersley. This research was supported in part by the U. S. Department of Energy under Grant No. DE-FG02-91ER40676.

References

1. K. G. Wilson, unpublished; quoted in L. Susskind, Phys. Rev. **D20**, 2619 (1979); G. 't Hooft, in *Recent Developments in Gauge Theories*, edited by G. 't Hooft, et al. (Plenum, New York, 1980).
2. See, for example, R. Dashen and H. Neuberger, Phys. Rev. Lett. **50**, 1897 (1983) 1897;
J. Kuti, L. Lin and Y. Shen, Phys. Rev. Lett. **61**, 678 (1988);
A. Hasenfratz, et al. Phys. Lett. **B199**, 531 (1987);
G. Bhanot and K. Bitar, Phys. Rev. Lett. **61**, 798 (1988).
3. S. Weinberg, Phys. Rev. **D19**, 1277 (1979);
L. Susskind, Phys. Rev. **D20**, 2619 (1979).
4. K Lane, *An Introduction to Technicolor*, Lectures given June 30–July 2 1993 at the Theoretical Advanced Studies Institute, University of Colorado, Boulder, published in “The Building Blocks of Creation”, edited by S. Raby and T. Walker, p. 381, World Scientific (1994); hep-ph/9401324.

5. R. S. Chivukula, *Models of Electroweak Symmetry*, NATO Advanced Study Institute on Quantum Field Theory Perspective and Prospective, Les Houches, France, 16–26 June 1998, hep-ph/9803219.
6. For a recent review, see K. Lane, *Technicolor 2000*, Lectures at the LNF Spring School in Nuclear, Subnuclear and Astroparticle Physics, Frascati (Rome), Italy, May 15–20, 2000, in preparation.
7. E. Eichten and K. Lane, Phys. Lett. **B90**, 125 (1980).
8. S. Dimopoulos and L. Susskind, Nucl. Phys. **B155** (1979) 237.
9. E. Eichten, I. Hinchliffe, K. Lane and C. Quigg, Rev. Mod. Phys **56**, 579 (1984); Phys. Rev. **D34**, 1547 (1986).
10. M. Golden, T. Han and G. Valencia, *Strongly-Interacting Electroweak Sector—Model Independent Approaches*, in Electroweak Symmetry Breaking and Beyond the Standard Model, ed. by T. Barklow, et al., hep-ph/9511206.
11. T. Barklow, in proceedings of the *International Symposium on Vector Boson Self-Interactions*, Los Angeles, CA 1995, ed. by U. Baur, et al., AIP 1996.
12. B. Holdom, Phys. Rev. **D24**, 1441 (1981); Phys. Lett. **B150**, 301 (1985);
T. Appelquist, D. Karabali, and L. C. R. Wijewardhana, Phys. Rev. Lett. **57**, 957 (1986);
T. Appelquist and L. C. R. Wijewardhana, Phys. Rev. **D36**, 568 (1987);
K. Yamawaki, M. Bando, and K. Matumoto, Phys. Rev. Lett. **56**, 1335 (1986);
T. Akiba and T. Yanagida, Phys. Lett. **B169**, 432 (1986).
13. K. Lane, *Technicolor Signatures at the High Energy Muon Collider*, Talk delivered at the workshop “Studies on Colliders and Collider Physics at the Highest Energies: Muon Colliders at 10 TeV to 100 TeV”, Montauk, Long Island, NY, 27 September–1 October 1999; hep-ph/9912526.
14. B. W. Lynn, M. E. Peskin, and R. G. Stuart, in Trieste Electroweak 1985, 213 (1985); M. E. Peskin and T. Takeuchi, Phys. Rev. Lett. **65**, 964 (1990);
A. Longhitano, Phys. Rev. **D22**, 1166 (1980); Nucl. Phys. **B188**, 118 (1981);
R. Renken and M. Peskin, Nucl. Phys. **B211**, 93 (1983);
M. Golden and L. Randall, Nucl. Phys. **B361**, 3 (1990);
B. Holdom and J. Terning, Phys. Lett. **B247**, 88 (1990);

- A. Dobado, D. Espriu, and M J. Herrero, Phys. Lett. **B255**, 405 (1990);
H. Georgi, Nucl. Phys. **B363**, 301 (1991).
15. Particle Data Group, http://pdg.lbl.gov/1999/contents_sports.html#stanmodeletc, p30.
16. R. S. Chivukula, S. B. Selipsky, and E. H. Simmons, Phys. Rev. Lett. **69**, 575 (1992);
R. S. Chivukula, E. H. Simmons, and J. Terning, Phys. Lett. **B331**, 383 (1994),
and references therein.
17. C. T. Hill, Phys. Lett. **B345**, 483 (1995).
18. C. T. Hill, Phys. Lett. **B266**, 419 (1991);
S. P. Martin, Phys. Rev. **D45**, 4283 (1992);
ibid **D46**, 2197 (1992); Nucl. Phys. **B398**, 359 (1993);
M. Lindner and D. Ross, Nucl. Phys. **B370**, 30 (1992);
R. Bönisch, Phys. Lett. **B268**, 394 (1991);
C. T. Hill, D. Kennedy, T. Onogi, H. L. Yu, Phys. Rev. **D47**, 2940 (1993).
19. M. Knecht and E. de Rafael, Phys. Lett. **B424**, 335 (1998); hep-ph/9712457;
T. Appelquist and F. Sannino, Phys. Rev. **D59**, 067702, 1999, hep-ph/9806409;
T. Appelquist, P. S. Rodrigues, and F. Sannino, Phys. Rev. **D60**, 116007 (1999),
hep-ph/9906555.
20. S. Weinberg, Phys. Rev. Lett. **18**, 507 (1967);
K. G. Wilson, Phys. Rev. **179**, 1499 (1969);
C. Bernard, A. Duncan, J. Lo Secco and S. Weinberg, Phys. Rev. **D12**, 792 (1975).
21. Y. Nambu, in *New Theories in Physics*, Proceedings of the XI International Symposium on Elementary Particle Physics, Kazimierz, Poland, 1988, edited by Z. Adjuk, S. Pokorski and A. Trautmann (World Scientific, Singapore, 1989), Enrico Fermi Institute Report EFI 89-08 (unpublished);
V. A. Miransky, M. Tanabashi and K. Yamawaki, Phys. Lett. **B221**, 177 (1989);
Mod. Phys. Lett. **A4**, 1043 (1989);
W. A. Bardeen, C. T. Hill and M. Lindner, Phys. Rev. **D41**, 1647 (1990);
C. T. Hill, Phys. Lett. **B266**, 419 (1991);
S. P. Martin, Phys. Rev. **D45**, 4283 (1992);
ibid **D46**, 2197 (1992); Nucl. Phys. **B398**, 359 (1993);

- M. Lindner and D. Ross, Nucl. Phys. **B370**, 30 (1992);
R. Bönisch, Phys. Lett. **B268**, 394 (1991);
C. T. Hill, D. Kennedy, T. Onogi, H. L. Yu, Phys. Rev. **D47**, 2940 (1993).
22. K. Lane and E. Eichten, Phys. Lett. **B222**, 274 (1989).
23. K. Lane and E. Eichten, Phys. Lett. **B352**, 382 (1995).
24. K. Lane, Phys. Rev. **D54**, 2204 (1996);
K. Lane, Phys. Lett. **B433**, 96 (1998).
25. E. Eichten and K. Lane, Phys. Lett. **B388**, 803 (1996); hep-ph/9607213;
E. Eichten, K. Lane, and J. Womersley, Phys. Lett. **B405**, 305 (1997); hep-ph/9704455;
E. Eichten, K. Lane, and J. Womersley, Phys. Rev. Lett. **80**, 5489 (1998); hep-ph/9802368.
26. K. Lane, Phys. Rev. **D60**, 075007 (1999), hep-ph/9903369. I refer to this paper as TCSM-1.
27. K. Lane and S. Mrenna, *Color-SU(3) Nonsinglet Technihadron Rates in the Technicolor Straw Man Model*, in preparation. I refer to this paper as TCSM-2.
28. T. Sjöstrand, Comp. Phys. Com. **82**, 74 (1994).
29. K. Lane and M. V. Ramana, Phys. Rev. **D44**, 2678 (1991).
30. The L3 Collaboration, *Search for Technicolor Production at LEP*, L3 Note 2428, submitted to the International Europhysics Conference High Energy Physics 99, Tampere, Finland 15–21 July 1999; <http://l3www.cern.ch/conferences/EPS99>.
31. The DELPHI Collaboration, DELPHI 2000-034 CONF 353, <http://delphiwww.cern.ch/teams/searches/moriond2000/technicolor/technicolor.html>
32. The CDF Collaboration, Phys. Rev. Lett. **84**, 1110 (2000).
33. The CDF Collaboration, Phys. Rev. Lett. **83**, 3124 (1999).
34. D. Toback *New Phenomena II: Recent Results from the Fermilab Tevatron* (for the CDF and DØ collaborations), Proceedings of the 35th Rencontres de Moriond: Electroweak Interactions and Unified Theories (Moriond 2000), hep-ex/0005020.

35. E. Farhi and L. Susskind, Phys. Rev. **D20**, 3404 (1979).
36. The CDF Collaboration, Phys. Rev. Lett. **82**, 3206 (1999).
37. The CDF Collaboration, (T. Affolder et al.), *Search for Second and Third Generation Leptoquarks Including Production via Technicolor Interactions in $p\bar{p}$ Collisions at $\sqrt{s} = 1.8$ TeV*, FERMILAB-PUB-00-073-E, Apr 2000, submitted to Physical Review Letters, hep-ex/0004003.
38. The CDF Collaboration, Phys. Rev. **D55**, R5263 (1997).
39. I am grateful to T. Handa of CDF for supplying these plots..
40. I am grateful to M. Narain of DØ for this plot.
41. ATLAS Detector and Physics Performance Technical Design Report, CERN/LHCC/99-14.
42. R. S. Chivukula, A. G. Cohen and E. H. Simmons, Phys. Lett. **B380**, 92 (1996), hep-ph/9603311;
M. Popovic and E. H. Simmons, Phys. Rev. **D58**, 095007 (1998), hep-ph/9806287.